arXiv:1503.07685v2 [math.OC] 20 Dec 2016

The matching problem between functional shapes via a BV-penalty term: a Γ-convergence result

B. Charlier *　　G. Nardi, A. Trouvé **

Abstract

In this paper we study a variant of the matching model between functional shapes introduced in [6]. Such a model allows to compare surfaces equipped with a signal and the matching energy is defined by the L^2-norm of the signal on the surface and a varifold-type attachment term.

In this work we study the problem with fixed geometry which means that we optimize the initial signal (supported on the initial surface) with respect to a target signal supported on a different surface. In particular, we consider a BV or H^1-penalty for the signal instead of its L^2-norm. Several numerical examples are shown in order to prove that the BV-penalty improves the quality of the matching. Moreover, we prove a Γ-convergence result for the discrete matching energy towards the continuous-one.

1 Introduction

Previous works. In [6], the authors introduce a new framework to study the matching problem for surfaces with boundary equipped with a signal (functional shapes or fshapes) called fshapes. New developments in non-invasive acquisition techniques suc as Magnetic Resonance Imaging (MRI) or Optical Coherence Tomography (OCT) allow to get geometric-functional data for several diseases (e.g., cortical thickness in the study of Alzheimer's disease or thickness of retina layers for the evolution of glaucoma). Then, new methods for the registration of fshapes are needed in medical imaging in order to describe anatomical variability and produce statistical estimate for several diseases.

The energy matching considered in [6] takes into account the L^2-norm of the signal on the surface and a varifold-type attachment term. Tools from geometric measure theory (currents, varifolds) are increasingly used in image processing [12, 8]. They actually allow to define a distance between two geometric objects in the setting of the measure theory. Moreover, because of their properties of compactness, they represent the good setting in order to define energies to minimize. However, such distances are defined in a weak sense and their computation can be very difficult. For this reason the model in [6] is developed in the setting of the Reproducing Kernel Hilbert Spaces (RKHS), which allows to easily compute a varifold distance. We refer to [6] and to Section 2 for more details.

The main difficulty of such a model arises from the fact that the position and the signal are minimized simultaneously. Now, the modification of one of these variables (position or signal) can be sufficient to get a local optimal configuration. Numerical simulations show that the gradient descent can be trapped in local minima where the signal has been strongly modified and the geometry has not.

---

[*] IMAG (UMR 5149), Université Montpellier, Campus du Triolet (CC051), Place Eugène Bataillon, 34095 Montpellier, France. Email: `benjamin.charlier@umontpellier.fr`

[**] CMLA, UMR 8536, Ecole Normale Supérieure de Cachan, 61 Avenue du Président Wilson, 94230 Cachan, France. Emails: `nardi,trouve@cmla.ens-cachan.fr`

This phenomenon is essentially due to two facts: the choice of the penalty term for the signal and the choice of Gaussian kernels to estimate the varifold-norm (see Example 3.4). The main object of this paper is to show that a BV-penalty term can strongly improve the matching results.

Contributions. In this work we consider the "functional" matching problem between (X, f) and a target fshape (Y, g). We consider the following three energies:

$$E(f) = R(f, X) + V((X, f), (Y, g)))$$

where $R(f, X)$ can be defined as

$$\begin{aligned} R(f, X) &= \tfrac{1}{2}\|f\|^2_{L^2(X)} \quad (L^2\text{-model})\,, \\ R(f, X) &= \tfrac{1}{2}\|f\|^2_{H^1(X)} \quad (H^1\text{-model})\,, \\ R(f, X) &= \|f\|_{BV(X)} \quad (\text{BV-model})\,. \end{aligned}$$

and the attachment term V is defined by using the varifold theory (see Section 2). The L^2-model represents the model introduced in [6].

We are interested here in the minimization problem with fixed geometry. This means that the optimization is made only with respect to the signal. In other words, the optimal fshape is supported on the initial surface X. We prove in particular an existence result for the optimal signal in the case of the BV and H^1-model. The existence result for the L^2-model is already proved in [6] theorem 6.

Afterwards, we define a discrete version of the problem by approximating the surface X by a sequence of triangulations. The continuous problem can be approximated by a sequence of discrete problems defined on some triangulations whose triangles's diameter goes to zero. Roughly speaking, smaller is the diameter of the triangles higher is the number of the vertices and, when the diameter goes to zero, the triangulation converges to the initial surface (with respect to the Hausdorff distance).

Concerning the definition of the discrete problems, the main issue is represented by the choice of the admissible triangulations. In fact, as X has a boundary, the triangulation and the surface need not be one-to-one. In this paper, we decided to work with the class of triangulations that cover the surface and whose surpassing part has small area.

Moreover, we must guarantee that the discrete solution is a "good" approximation of the continuous local minimum. This can be proved by the Γ-convergence theory, that is a natural notion of convergence of functionals allowing to justify the passage from discrete to continuous problems. In particular, in the case of minimization problems, the Γ-convergence guarantees also the convergence (in some sense) of the discrete minima towards the continuous-one.

We prove a Γ-convergence result showing that the minimum of the discrete problem is close to the minimum of the continuous problem if the diameter of the triangles is small. The main issue to get such a result arises from the fact that the discrete problems and the continuous problem are not defined on the same geometric support. Now, in order to get the Γ-convergence result we need some hypothesis on the triangulations which guarantee the convergence of the areas. There is in fact a famous example (see Schwartz's lantern example in [23] p. 354) proving that the area of the triangulations described above needs not to converge to the area of X.

Following [19], we point out the suitable properties a sequence of triangulations should verify to guarantee the convergence of the areas. To this end the angle between the normal to the triangulations and the respective (in the sense of the projection on the surface) normal to the surface has to go to zero. For every penalty (L^2, H^1, BV), previous condition on the triangulations allows to prove the Γ-convergence result for the respective energy.

This kind of condition is involved in the numerical study of several problems defined on surfaces (e.g., Laplace-Beltrami operator). Then our result can be useful behind the matching model for fshapes.

Finally, we show some numerical examples to compare the different models. These examples actually point out that the BV-model strongly improves the matching result.

Relationship with [6]. The problem studied in this work corresponds to the model presented in [6] with different signal-penalty term and fixed geometry. In this paper, we point out the influence of the penalty term on the quality of the matching and the properties needed to get a Γ-convergence result. The present work represents a important step in order to improve the general model presented in [6].

Moreover, studying the problem with fixed geometry does not make the problem trivial. In fact, we perform the matching between two different fshapes that are not supported on the same surface. Such a geometric difference is taken into account by the varifold attachment term. Then, the influence of the penalty term and its interaction with the varifold term is a interesting problem to study.

In particular, we address the problem of the existence of a solution, the discretization of the problem and a related Γ-convergence result. These problems represent are needed to get a similar result in the general case of fshape (i.e., the surface X can vary). The effect of the penalty term on the geometric optimization will be addressed in a future work.

Structure of the paper. In Section 2 we remind the definition of varifold and the RKHS framework used in [6] in order to estimate the varifold norm. In Section 3 we introduce the three models (L^2, H^1, BV) studied in this paper and prove the existence result for the BV and H^1-models. In Section 4 we define the class of admissible triangulations and a condition on the angles between the respective normals in order to get the convergence of the area. In Section 5 we define, in the setting of the finite elements method, a discrete version of the energies introduced in Section 3. Section 6 is devoted to the definition of the discrete problems and the results of Γ-convergence. Section 7 shows several numerical examples in order to compare the different models. Finally, in the Appendix, we recall the definition of the BV functions on manifolds and prove that such functions may be approximated by C^1 functions.

2 The functional varifold setting

In the following we assume that :

Hypothesis 1. X is a 2-surface of $\mathbb{R}^3$ with boundary. X is smooth (C^2 at least) oriented, connected and compact.

The boundary of X is denoted by ∂X and the interior is denoted X_0. The smoothness condition in Hypothesis 1 means that X_0 is a two dimension smooth manifold and ∂X is a one dimensional manifold of the same regularity. In this section we remind the main tools needed to set the model introduced in [6].

Definition 2.1 **(fshape).** We define a fshape as a couple (X, f) where X is a surface verifying Hypothesis 1 and $f : X \to \mathbb{R}$ is a signal defined on X.

We denote by $L^p(X)$, $W^{1,p}(X)$, and $BV(X)$ the usual Lebesgue, Sobolev and bounded variation functional spaces defined on the surface X (see Appendix 9 for details). In order to define a suitable attachment term we remind the definition of functional varifold. The space of continuously differential functions defined on a norm space E and vanishing at infinity is denoted $C_0^1(E)$.

Definition 2.2 (fvarifolds). A 2-dimensional functional varifold (fvarifold) is any linear form belonging to $(C_0^1(\mathbb{R}^3 \times G(3,2) \times \mathbb{R}))'$, the dual of the space of real valued continuous functions vanishing at infinity. We denote by $G(3,2)$ the Grassmannian of the non-oriented 2-dimensional linear subspaces of $\mathbb{R}^3$. This space (diffeomorphic to the projective space $P^1(\mathbb{R}^3)$) has a structure of smooth manifold and can be equipped with a smooth distance

$$d(S,T) = (2(1 - \langle \boldsymbol{n}_S, \boldsymbol{n}_T \rangle^2))^{1/2}$$

where $\boldsymbol{n}_S$ and $\boldsymbol{n}_T$ are respectively unit normal vectors to S and T in $G(3,2)$.

In particular, we can associate a fvarifold with a fshape (X, f) by setting

$$\mu_{(X,f)}(\varphi) = \int_X \varphi(x, T_x X, f(x)) d\mathcal{H}^2(x) \quad \forall \varphi \in C_0^1(\mathbb{R}^3 \times G(3,2) \times \mathbb{R}),$$

whrere $d\mathcal{H}^2$ is the 2-dimensional Hausdorff (or volume) measure. Remark that, according to Theorem 1 p. 49 in [15], such a functional is represented by a measure on $C_0^1(\mathbb{R}^3 \times G(3,2) \times \mathbb{R})$. Next lemma is very usefull in the following. It can be easily shown by the previous definition of fvarifold.

Lemma 2.3. Let $\{X_h\}$ be a sequence of surfaces such that $\mathcal{H}^2(X_h) \to 0$. Then $\mu_{(X_h,f_h)}$ converges to the null varifold for every sequence $\{f_h\}$ of signals.

We refer to [22] for more properties of varifolds and to [6] for more properties of functional varifolds.

In [6], the authors evaluate the varifold norm by an embedding into a RKHS generated by Gaussian kernels. We refer to [24] for an introduction to RKHS theory and to Section 3.2.2 in [6] for a general discussion on the construction of a suitable RKHS for our framework.

Following [6], we consider W as the RKHS associated with the positive kernel

$$k((x, T_1, f_1), (y, T_2, f_2)) = k_e(x_1, x_2) \otimes k_t(T_1, T_2) \otimes k_f(f_1, f_2)$$

where k_e, k_t, k_v are some positive kernels on $\mathbb{R}^3$, the Grassmannian, and $\mathbb{R}$, respectively. In our applications we use the following smooth Gaussian kernels

$$k_e(x,y) = e^{-\frac{\|x_1 - x_2\|^2}{\sigma_e^2}}, \; k_t(T_1, T_2) = e^{-\frac{2(1 - \langle \boldsymbol{n}_{T_1}, \boldsymbol{n}_{T_2} \rangle^2)}{\sigma_t^2}}, \; k_f(a,b) = e^{-\frac{|f_1 - f_2|^2}{\sigma_f^2}} \tag{2.1}$$

where $\sigma_e, \sigma_t, \sigma_f$ are three positive constants and $\boldsymbol{n}_{T_k}$ represents the unit normal vector to T_k. Remark that, we define a kernel on the Grassmannian by identifying the linear space (plane) with its normal space (line).

Then, W is continuously embedded in $C_0^1(\mathbb{R}^3 \times G(3,2) \times \mathbb{R})$ (see Proposition 3 in [6]), and we can define a continuous map

$$i^* : (C_0^1(\mathbb{R}^3 \times G(3,2) \times \mathbb{R}))' \to W' .$$

In particular, for every $\mu \in (C_0^1(\mathbb{R}^3 \times G(3,2) \times \mathbb{R}))'$ we have

$$\|\mu\|_{W'} \leqslant \sup \{\mu(\varphi) \, : \, \|\varphi\|_{C_0^1(\mathbb{R}^3 \times G(3,2) \times \mathbb{R})} \leqslant 1\} , \tag{2.2}$$

where, by an abuse of notation, we denote $i^*(\mu)$ by μ. Moreover, as W and W' are Hilbert spaces, every functional $\mu \in W'$ can be represented by an element of W via the isometry $K_W : W' \to W$ given by

$$\langle K_W \mu, \varphi \rangle_W = \mu(\varphi) \quad \forall \varphi \in W\,, \ \ \forall \mu \in W'$$

so that, for every fvarifold, we get

$$\|\mu\|_{W'} = \|K_W \mu\|_W \quad \forall \mu \in (C_0^1(\mathbb{R}^3 \times G(3,2) \times \mathbb{R}))'\,.$$

In particular, the kernel represents every Dirac delta functional, which means that

$$K_W \delta_{(x_1,V_1,f_1)} \,:\, (x,V,f) \mapsto k((x_1,V_1,f_1),(x,V,f))$$

for every $(x_1,V_1,f_1) \in \mathbb{R}^3 \times G(3,2) \times \mathbb{R}$. Then

$$\langle \delta_{(x_1,V_1,f_1)}, \delta_{(x_2,V_2,f_2)} \rangle_{W'} = k_e(x_1,x_2) k_t(V_1,V_2) k_f(f_1,f_2)\,, \tag{2.3}$$

for every $(x_1,V_1,f_1),(x_2,V_2,f_2) \in \mathbb{R}^3 \times G(3,2) \times \mathbb{R}$, so that, for every couple of fshape $(X,f),(Y,g)$ we get

$$\langle \mu_{(X,f)}, \mu_{(Y,g)} \rangle_{W'} = \int_X \int_Y k_e(x,y) k_t(T_x X, T_y Y) k_f(f(x),g(y))\, d\mathcal{H}^2(x) d\mathcal{H}^2(y)\,. \tag{2.4}$$

Moreover, $\|\mu_{(X,f)} - \mu_{(Y,g)}\|_{W'}$ is a distance between fshapes which can be easily computed using (2.4). Such a framework (fvarifolds and RKHS dual norm) is used in [6] and in the present work in order to define an attachment term between fshapes.

3 The matching energy: an existence result

In this section we define the matching energy between two fshapes and we prove an existence result for the optimal solution.

Let be (Y,g) a target fshape. We consider the following three energies defined for a generic fshape (X,f):

$$E(f) = R(f,X) + \frac{1}{2}\|\mu_{(X,f)} - \mu_{(Y,g)}\|^2_{W'} \tag{3.1}$$

where $R(f,X)$ can be defined as

$$\begin{aligned} R(f,X) &= \tfrac{1}{2}\|f\|^2_{L^2(X)} \quad && (L^2\text{-model})\,, \\ R(f,X) &= \tfrac{1}{2}\|f\|^2_{H^1(X)} \quad && (H^1\text{-model})\,, \\ R(f,X) &= \ \ \|f\|_{BV(X)} \quad && (\text{BV-model})\,. \end{aligned}$$

In particular, we aim to solve the minimization problem

$$\inf_f E(f)$$

where the infimum is taken on the respective space ($L^2(X), H^1(X)$ or $BV(X)$). In this section we state and prove an existence result for such a problem. In the case of the BV-model and H^1-model the proofs are very similar so we prove the result for the BV-model and we indicate how it can be adapted to the H^1-case.

We remind that we optimize only with respect to the signal which implies that the initial configuration and the optimal one have the same geometric support. However, the geometry is taken into account in the attachment term.

As pointed out in the introduction such a problem is not trivial and strongly depends on the choice of the penalty term R. In fact, as we work with Gaussian kernels, an oscillating signal can be more economic in terms of energy E (see Example 3.4). This is due essentially to the fact that $e^{-|a-b|^2}$ is small if $|a-b|$ is large. The choice of a penalty term which takes into account the gradient of the signal prevents this kind of optimal configurations.

A sequence $(\mu_h)_h$ of W is said to weak-$*$ converge to $\mu \in W$ if

$$\lim_{h\to 0} \mu_h(\varphi) = \mu(\varphi), \quad \forall \varphi \in C_0^1(\mathbb{R}^3 \times G(3,2) \times \mathbb{R}).$$

In that case we write $\mu_h \overset{*}{\rightharpoonup} \mu$. The following Lemma links the pointwise convergence of a signal and the weak-$*$ convergence of fvarifolds. It can be easily proved using the definition of varifold and applying the dominated convergence to (2.4).

Lemma 3.1. If $f_h \to f$ a.e. on X then $\mu_{(X,f_h)} \overset{*}{\rightharpoonup} \mu_{(X,f)}$. Moreover,

$$\|\mu_{(X,f)}\|_{W'} = \lim_{h\to 0} \|\mu_{(X,f_h)}\|_{W'}\,.$$

3.1 The L^2-model

The L^2-model is studied in [6] part I. The authors consider the matching energy

$$E(f) = \frac{\gamma_f}{2}\|f\|^2_{L^2(X,\mathbb{R})} + \frac{\gamma_W}{2}\|\mu_{(X,f)} - \mu_{(Y,g)}\|^2_{W'} \tag{3.2}$$

where γ_f, γ_W are two positive constants. They prove the following general result :

Theorem 3.2 (Proposition 7 in [6])**.** Let X, Y be two finite volume bounded 2-rectifiable subsets of $\mathbb{R}^3$. Let us assume that W is continuously embedded in $C_0^2(\mathbb{R}^3 \times G(3,2) \times \mathbb{R})$ and $g \in L^2(Y)$.

If the ratio γ_f/γ_W is large enough, then there exists at least one solution to the minimization problem

$$\inf_{f\in L^2(X)} E(f)$$

and every minimizer belongs to $L^\infty(X)$. Moreover, if X is a C^p-surface and $W \hookrightarrow C_0^m(\mathbb{R}^3 \times G(3,2) \times \mathbb{R})$ with $m \geqslant \max\{p, 2\}$, then every minimizer belongs to $C^{p-1}(X)$.

Finally, there exists a constant $C > 0$ (independent of X and Y) such that, every minimizer verifies

$$\|f\|_{L^\infty(X)} \leqslant C\frac{\gamma_W}{\gamma_f}(\mathcal{H}^2(X) + \mathcal{H}^2(Y))\,. \tag{3.3}$$

We point out that, for every minimizing sequence $(f_h)_h$, a bound on $E(f_h)$ guarantees only the L^2-weak compactness for the signals, which is not enough to get the semi-continuity of the varifold term (see Lemma 3.1). To avoid this problem the authors relax the problem to the class $\mathcal{M}^X$ defined as it follows:

Definition 3.3. $\mathcal{M}^X$ is the class of the Borel finite measures ν on $\mathbb{R}^3 \times G(3,2) \times \mathbb{R}$ such that

$$\int \varphi(x,V)d\nu(x,V,f) = \int_X \varphi(x,T_xX)d\mathcal{H}^2(x) \quad \forall\,\varphi \in C_c(\mathbb{R}^3 \times G(3,2))\,.$$

Note that $\mu_{(X,f)} \in \mathcal{M}^X$ for every fshape (X,f).

In this framework, they relax the energy E to the following energy

$$\tilde{E} : \mathcal{M}^X \to \mathbb{R}\ , \quad \tilde{E}(\nu) = \frac{\gamma_f}{2} \int |f|^2 d\nu + \frac{\gamma_W}{2} \|\nu - \mu_{(Y,g)}\|^2_{W'}\,. \tag{3.4}$$

It holds that

$$E(f) = \tilde{E}(\mu_{(X,f)})\,. \tag{3.5}$$

This allows one to get compactness in the setting of measures by using the Prokhorov's theorem. Moreover, it can be shown that the minimizing measure ν^* of $\tilde{E}$ is actually associated with a fshape, so that $\nu^* = \mu_{(X,f^*)}$ for some $f^* \in L^2(X)$. The proof relies on the Implicit Function Theorem which needs the hypothesis on γ_f/γ_W. We refer to Proposition 7 and Lemma 2 in [6] for more details.

Such a model has two main issues. Firstly the existence result depends on the weights used to define the energy. Moreover, the L^2 penalty does not prevent from some oscillating configurations for the optimal signal. Next example, which is similar to simulations in [6] Section 9.1, points out these facts.

Example 3.4. We consider the two fshapes shown in Figure 1: two bended smooth stars both lying on the cylinder $\{(x, y, z) \in \mathbb{R}^3 | x^2 + y^2 = 1\}$. The source fshape is a fat star with constant signal equals to zero composed of 22880 vertices (45171 triangles). The target fshape is a thin star with a signal taken from "Lena" picture widely use in the image processing community (the signal has been normalize to range between 0 and 1) composed of 4056 vertices (7744 triangles).

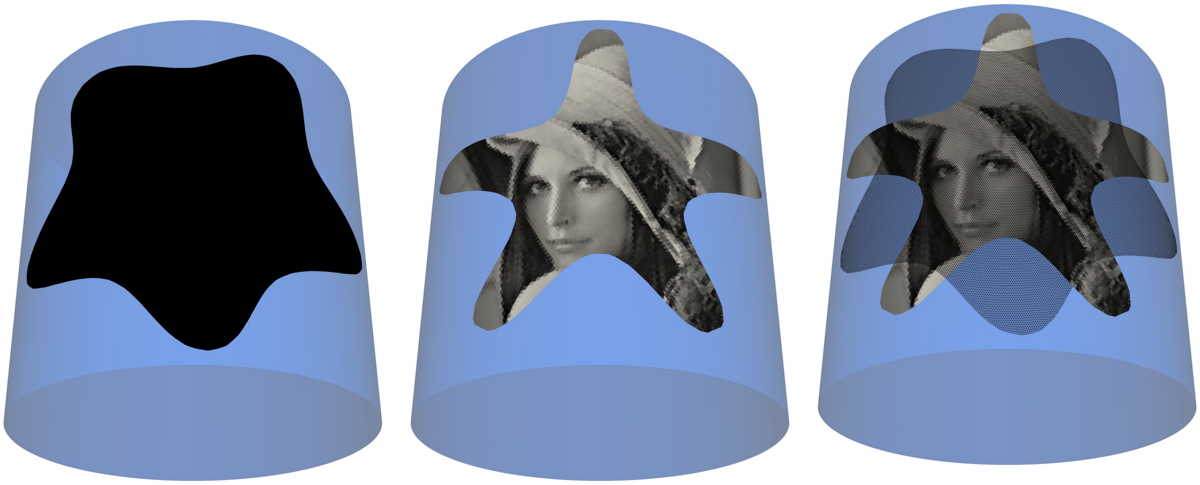

(a) Source $(X, 0)$ (b) Target (Y, g) (c) Relative position (mesh view)

Figure 1: The initial fshape is a fat smooth star 1a and the target fshape (Y, g) is a thin star with Lena picture as grey level signal 1b (black is 0 and white is 1). Remark the pixel effect due to the $P0$ discretization (see Section 5). The blue cylinder is just drawn to help to see the perspective.

The two fshapes are "overlapping" although we emphasis that they do *not* contain the same number vertices and do *not* share any vertices (see Figure 1c). In order to minimize the varifold norm appearing in the matching energy (3.2), the fshape source has to be carried with a Lena signal on the overlapping part of the two fshapes. On the remaining part of the source, the optimal signal is determined by the penalty term and it should ideally remain to zero (no information added).

We use the `fshapesTk` software [7] to minimize a discrete version of (3.2). Thorough details about the discrete energy is given below. We choose $\gamma_W = 1$ since the balance between terms is only determine by the ratio γ_f/γ_W. We recognize the same behaviour as in the example of [6] Section 9.1: the optimal signal is strongly depending on γ_f and is oscillating on the non overlapping part (the Moiré pattern visible at the end of the branches on Figures 2b, 2c and 2d). The intensity of the oscillations as well as the contrast of the optimal signal depend on the value of the parameter γ_f as shown by Figures 2b and 2c. As discussed in [6], a possible trick improving the quality of the optimal signal is to smooth the gradient used along the gradient descent (see Figure 2d).

As pointed out at the beginning of this section, this essentially depends on the behavior of Gaussian kernels. As shown further, this kind of configurations is avoided by the BV-model.

3.2 The BV-model

We consider the following energy

$$E(f) = \|f\|_{BV(X)} + \frac{1}{2}\|\mu_{(X,f)} - \mu_{(Y,g)}\|^2_{W'} \tag{3.6}$$

where (Y, g) is a target fshape. The H^1-model can be studied in a similar way (see Remark 3.6). We are interested in solving the following problem

$$\inf_{f\in BV(X)} E(f)\,. \tag{3.7}$$

We prove now the existence of a solution to problem (3.7).

Theorem 3.5. Problem (3.7) admits at least one solution.

Proof. Let $(f_h)_h$ be a sequence of $BV(X)$ minimizing for E. We can suppose that $\|f_h\|_{BV(X)}$ is uniformly bounded and, by the compactness theorem for BV-functions, $(f_h)_h$ converges (up to a subsequence) to some $f \in BV(X)$ with respect to weak-$*$ topology. This implies in particular that (up to a subsequence) $f_h \to f$ a.e. on X. The result ensues by remarking that the fvarifold norm is lower semicontinuous with respect to the a.e.-convergence (Lemma 3.1), and that the BV-norm is lower semicontinuous with respect to the weak-$*$ topology. $\square$

Remark 3.6 (The H^1-model). We point out that we get the same result if we consider signals belonging to $H^1(X)$ instead of $BV(X)$. This follows from the fact that the unity ball of $H^1(X)$ is compact with respect to the weak topology. Moreover, $H^1(X)$ is compactly embedded in $L^2(X)$, which implies in particular (up to a subsequence) the a.e.-convergence of the minimizing sequence.

4 Surfaces and triangulations

In this section we remind the main properties of triangulations and describe how to compare a signal defined on a surface with a signal on a related triangulation.

4.1 Triangulations of a surface

We start by stating some general notions about triangulations related to the surface X. We remind that X verifies Hypothesis 1. Following [1, 21, 20] we give the following definition of triangulation:

Definition 4.1 (Triangulations). A triangulation $\mathcal{T}$ is a two-dimensional manifold (with boundary) consisting of a finite set $\Delta_{\mathcal{T}}$ of topological triangles such that:

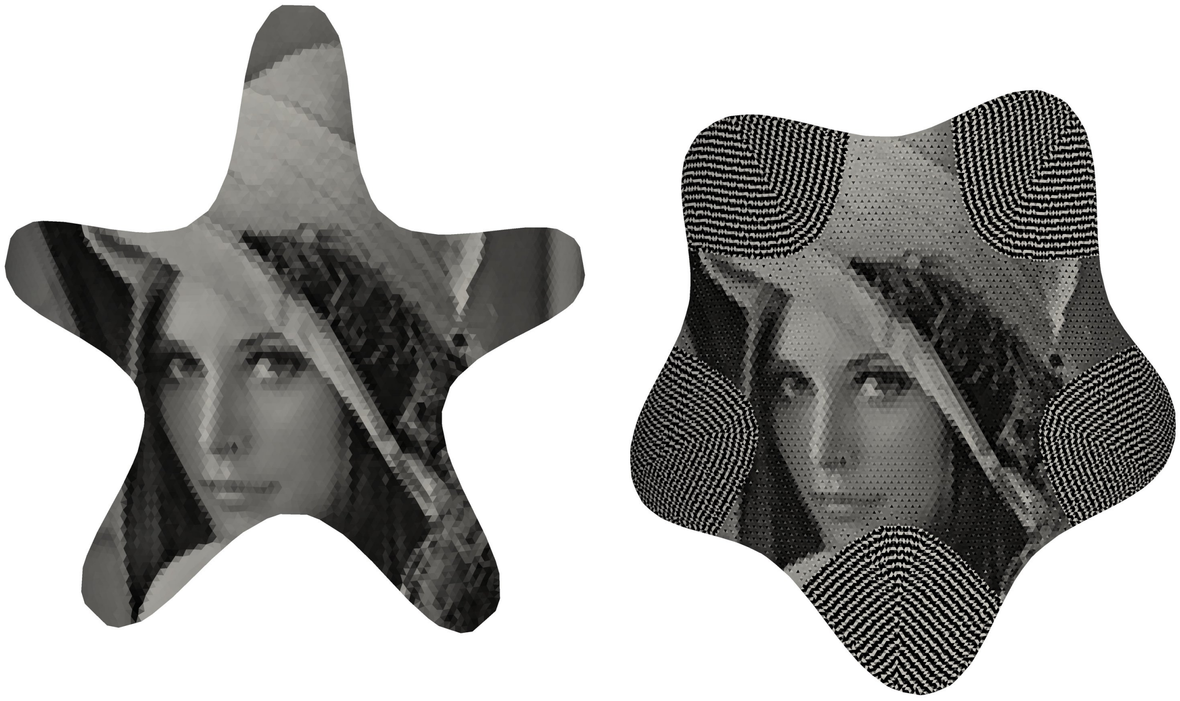

(a) The target (Y, g)

(b) Optimal fshape (X, f^*) with $\gamma = 0.1$.

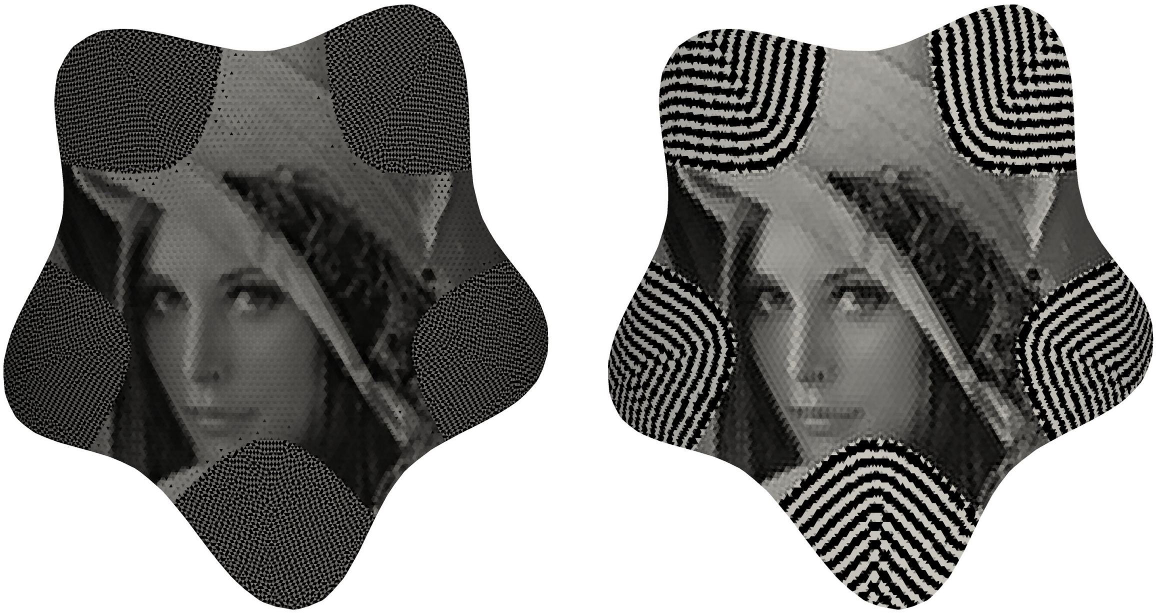

(c) Optimal fshape (X, f^*) with $\gamma = 1$

(d) Optimal fshape (X, f^*) with $\gamma = 0.01$ and with a smoothed gradient descent.

Figure 2: Results for the L^2 penalty: *en face* view of the target (Figure 2a) and of the optimal signals f^* defined on X (Figures 2b, 2c and 2d). The optimal signal f^* is obtained by minimization of the discrete version of the functional (3.2) with various parameters.

1. any point $p \in \mathcal{T}$ lies in at least one triangle $T \in \Delta_{\mathcal{T}}$;
2. each point $p \in \mathcal{T}$ has a neighbourhood that intersects only finitely many triangles $T \in \Delta_{\mathcal{T}}$;
3. the intersection of any two non-identical triangles $T, T' \in \Delta_{\mathcal{T}}$ is either empty, or consists of a common vertex, or of a simple arc that is an edge of each of the two triangles.

In the following we denote by T a generic triangle of $\Delta_{\mathcal{T}}$ and by $\partial\mathcal{T}$ the boundary of the manifold $\mathcal{T}$. We call vertices of $\mathcal{T}$ the set of vertices of the triangles $T \in \Delta_{\mathcal{T}}$. Finally, we define

$$\operatorname{diam}_{\mathcal{T}} \doteq \max_{T \in \Delta_{\mathcal{T}}} \{\operatorname{diam}(T)\}, \tag{4.1}$$

i.e. $\operatorname{diam}_{\mathcal{T}}$ is the supremum of all the diameters of the triangles composing $\mathcal{T}$.

Definition 4.2 (**C-Regular triangulation).** We denote by $\mathbb{T}_C$ the set of triangulations $\mathcal{T}$ such that there exists a constant C such that

$$\frac{h_T}{\rho_T} \leqslant C \qquad \forall T \in \Delta_{\mathcal{T}} \tag{4.2}$$

where h_T is the diameter of T and ρ_T is the diameter of the sphere inscribed in T.

We define the distance function as

$$\forall x \in \mathbb{R}^3 \ , \quad d_X(x) \doteq d(x, X) = \inf_{y \in X} |x - y| \, .$$

For every $x \in \mathbb{R}^3$, we call (if it exists) projection of x on X every point $\pi_X(x) \in X$ such that $d_X(x) = |x - \pi_X(x)|$.

Definition 4.3 (Tubular neighborhood)**.** Let X be a surface satisfying Hypothesis 1. We denote by $U_r(X)$ a subset of $\mathbb{R}^3$ of the form

$$U_r = \{ \ x \in \mathbb{R}^3 \mid d_X(x) < r \ \}$$

such that every point $x \in U_r$ admits a unique projection $\pi_X(x) \in X$. We refer to [10] for the proof of the existence of such a tubular neighborhood for some $r > 0$.

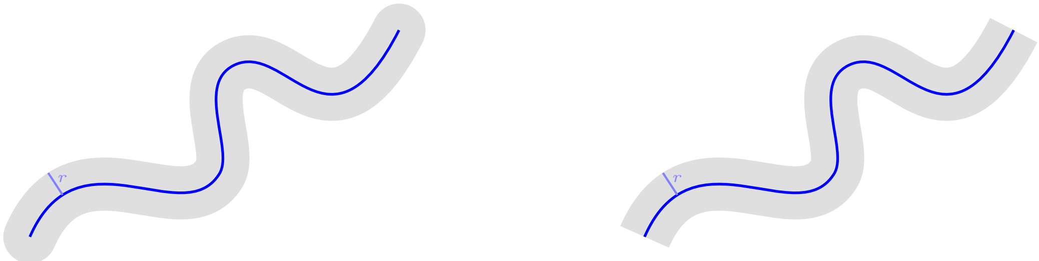

(a) The tubular neighborhood $U_r(X)$

(b) The set $\mathcal{N}_r(X)$

Figure 3: A surface X sketches by a blue curve and its tubular neighborhood.

We remark that the projection is not injective on the set $U_r(X)$ but only on the following subset

$$\mathcal{N}_r(X) \,=\, \{x + t\boldsymbol{n}_X(x) \,:\, t \in]-r, r[,\, x \in X\} \tag{4.3}$$

where we denote by $\boldsymbol{n}_X(x)$ the unit normal vector to X at x (see Figure 3). Remark that normal vector can be defined on ∂X by continuity. We also point out that $d_X \in C^2(\mathcal{N}_r(X))$. If $x \in \mathcal{N}_r(X)$ then its projection on the surface is defined by the following equation:

$$x = \pi_X(x) + d_X(x)\boldsymbol{n}_X(\pi_X(x))\,. \tag{4.4}$$

As pointed out in the introduction, because of the curvature of ∂X, we can not assume that a triangulation, obtained by the sampling of some points of X, is in bijection with the surface. Then, in order to correctly define a discrete setting, we introduce a particular class of triangulations. Before stating the definition we need the following notations : let $r > 0$ and for every triangulation $\mathcal{T}$ belonging to the tubular neighborhood $U_r(X)$ of a surface X we denote

$$\mathcal{T}^{\text{in}} = \mathcal{T} \cap \mathcal{N}_r(X) \quad \text{ and } \quad \mathcal{T}^{\text{out}} = \mathcal{T} \cap \mathcal{N}_r(X)^c\,.$$

Definition 4.4 (**h-admissible triangulations for a surface).** Let $h > 0$. We say that a triangulation $\mathcal{T}$ is h-admissible for the surface X if the following properties hold

(*i*) $\mathcal{T}$ lies in $U_h(X)$;

(*ii*) $\mathcal{T}$ lies in $\mathcal{N}_h(X^{+\eta})$ for some $\eta > 0$, where $X^{+\eta}$ is an extension of X defined in (9.14);

(*iii*) $\mathcal{T}^{\text{in}}$ and X are in one-to-one correspondence through π_X;

(*iv*) $\mathcal{H}^2(\mathcal{T}^{\text{out}}) = O(h)$.

(*v*) $\text{diam}_{\mathcal{T}} = O(h)$ defined in (4.2)

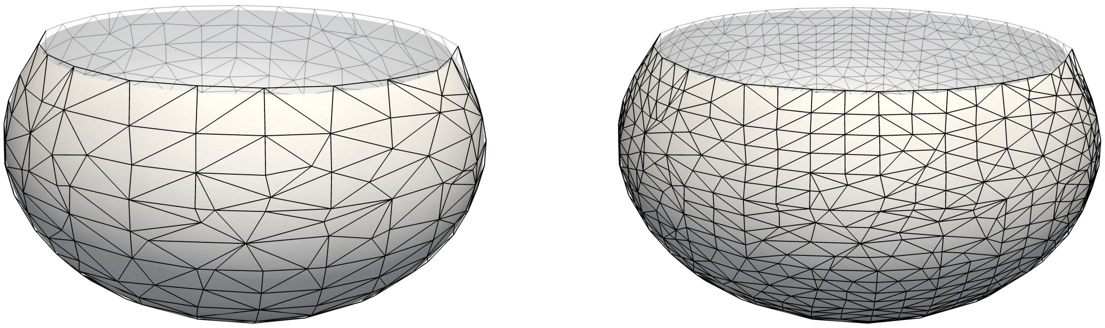

(a) h_1-admissible triangulation $\mathcal{T}_{h_1}$ for X (b) h_2-admissible triangulation $\mathcal{T}_{h_2}$ for X

Figure 4: A surface X with boundary (solid grey) and two admissible triangulations (black lines) with $h_1 > h_2$. The area of $\mathcal{T}^{\text{out}}_{h_2}$ (*i.e.* the upper part of triangulation exceeding X) is smaller than $\mathcal{T}^{\text{out}}_{h_2}$.

Previous definition guarantees that every h-admissible triangulation $\mathcal{T}$ can be decomposed in two parts: $\mathcal{T} = \mathcal{T}^{\text{in}} \cup \mathcal{T}^{\text{out}}$. The first-one, $\mathcal{T}^{\text{in}}$, lies in $\mathcal{N}_h(X)$ and is in bijection with X. We can define a partition of X by considering the family $\{\hat{T}_i\}$ defined by

$$\hat{T}_i = \pi_X(T_i \cap \mathcal{N}_h(X)) \quad \forall\, T_i \in \mathcal{T}\,.$$

The second-one, $\mathcal{T}^{\text{out}}$, lies outside $\mathcal{N}_h(X)$ and condition (iv) guarantees that its area is small (see Figure 4).

Remark 4.5. In general, an inscribed triangulation (in the sens of [19]) is not in bijection with a surface with smooth boundary through the normal projection. The bijectivity can fail close to ∂X because of the curvature of ∂X as depicted in Figure 5a. Locally, the normal projection of ∂X on a hyper-plane needs not to be a line. In that case, it is not possible to project ∂X on an edge of a triangle.

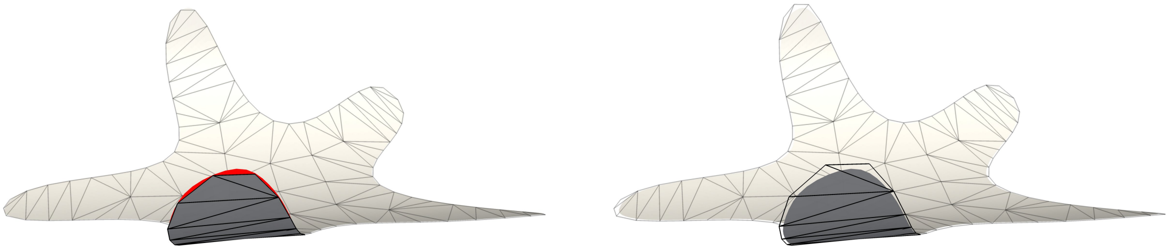

(a) Inscribed triangulation $\mathcal{T}_1$ for X

(b) An h-admissible triangulation $\mathcal{T}_2$ for X

Figure 5: The surface X is a bended smooth star (solid grey) as in Figure 1b. Two triangulations (black lines) are pictured. Figure 5a the triangulation $\mathcal{T}_1$ is not in one-to-one correspondence with X through the projection map (for instance the part of the smooth star in red exceed the triangulation). Figure 5b the subset $\mathcal{T}_2^{\text{in}}$ of $\mathcal{T}_2$ is in one-to-one correspondance with X.

Remark 4.6 (Real data). We point out that the previous definition is slightly different from the usual notion of triangulation associated with a manifold. We actually do not suppose that the vertices of the $\mathcal{T}$ belong to the manifold X. See Figure 5b.

Such a generalization corresponds better to the features of the experimental images. In fact, the original images (OCT, functional MRI) are modified (segmentation, deblurring, denoising) in order to improve their quality and to be used for the numerical tests. Then, the real data that we use represent an approximation of the real objects we want to compare, and, moreover, can contain some noise. By considering a set of triangulations whose vertices do not belong to X, the results set in this paper are more adequate to such a situation.

4.2 Convergence of areas

We remind that the Hausdorff distance between two surfaces $X, Y \subset \mathbb{R}^3$ is defined as

$$d_{\mathcal{H}}(X,Y) = \max\Big\{\sup_{x\in X} d_Y(x), \sup_{y\in Y} d_X(y)\Big\}.$$

If $\mathcal{T}$ is an h-admissible triangulation of X for some $h < 0$ then property (i) of Definition 4.4 implies that $d_{\mathcal{H}}(X,\mathcal{T}) < h$. Unfortunately, the convergence with respect to Hausdorff distance does not imply the convergence of the areas. A counterexample is given by the Schwartz's lantern (see [23] page 354). In the following we remind a result from [19] giving a sufficient condition in order to have the convergence of the areas.

Definition 4.7 (Angle between normals). Let $h > 0$. Assume that $\mathcal{T}$ is an h-admissible triangulation for X. For every $x \in \mathcal{T}^{\text{in}}$ we define the angle α_x as follows

- if x belongs to the interior of some triangle, then α_x is the angle belonging to $[0,\pi/2]$ between the two normals $\boldsymbol{n}_X(\pi_X(x))$ and $\boldsymbol{n}_{\mathcal{T}}(x)$;
- if x belongs to an edge of a triangle, then α_x is the biggest angle (belonging to $[0,\pi/2]$) between $\boldsymbol{n}_X(\pi_X(x))$ and the normals of the triangles containing x.

In the following we set

$$\alpha_{\max} \doteq \sup_{x\in\mathcal{T}^{\text{in}}} \alpha_x \,.$$

Lemma 4.8. *Let $h>0$ and $\mathcal{T}$ be an h-admissible triangulation for X. We have*

$$|\mathcal{H}^2(X)-\mathcal{H}^2(\mathcal{T}^{\text{in}})| = O(\alpha_{\max}^2 + d_{\mathcal{H}}(X,\mathcal{T}))$$

as $\alpha_{\max}^2, d_{\mathcal{H}}(X,\mathcal{T}) \to 0$ when $h\to 0$, where $\alpha_{\max}$ is introduced in Definition 4.7.

Proof. For every $x\in X$ we consider on the tangent space T_xX the basis $\mathcal{B}(x)=\{e^1(x),e^2(x)\}$ given by the two principal directions. We denote by $\kappa_1(x)$ and $\kappa_2(x)$ the principal curvatures of X at x. Similarly, for every $x\in X$ we can consider the basis $\tilde{\mathcal{B}}(x)=\{e^1(x),e^2(x),\boldsymbol{n}_X(x)\}$ for $\mathbb{R}^3$.

Consider the differential $D\pi_X:\mathbb{R}^3\to T_{\pi_X(x)}X$ of π_X. Note that, for every $x\in\mathcal{N}_h(X)$, we have $D\pi_X(x)(v)=0$ for every variation v in the direction $\boldsymbol{n}_X(\pi_X(x))$ orthogonal to $T_{\pi_X(x)}X$. So, we should just consider the tangential variations in order to calculate the Jacobian of the projection. In [19] it is proved that for any $x\in U_h(X)$ and v parallel to $T_{\pi_X(x)}X$ we have

$$D\pi_X(x)(v) = \Big(I_{\restriction_{T_{\pi_X(x)}X}} - \varepsilon_x d_X(x) D\boldsymbol{n}_X(\pi_X(x))\Big)^{-1} v$$

And the matrix of $D\pi_X(x)$ written with respect to the basis $\tilde{\mathcal{B}}(\pi_X(x))$ and $\mathcal{B}(\pi_X(x))$ is

$$D\pi_X(x) = \begin{pmatrix} \frac{1}{1+d_X(x)\varepsilon_x\kappa_1(\pi_X(x))} & 0 & 0 \\ 0 & \frac{1}{1+d_X(x)\varepsilon_x\kappa_2(\pi_X(x))} & 0 \end{pmatrix}$$

where $\varepsilon_x = \langle \frac{\pi_X(x)-x}{\|\pi_X(x)-x\|}, \boldsymbol{n}_X(\pi_X(x))\rangle \in \{-1,+1\}$.

Let now $A\subset\mathcal{T}^{\text{in}}$ be a subset of a triangle of $\mathcal{T}$. This implies that the Jacobian of the projection on X restricted to A is given by

$$\det(D_{\restriction_A}\pi_X)(x) = \frac{\cos\alpha_x}{(1+d_X(x)\varepsilon_x\kappa_1(\pi_X(x)))(1+d_X(x)\varepsilon_x\kappa_2(\pi_X(x)))} \quad \forall x\in A\,.$$

We have $\cos\alpha_x = 1+O(\alpha_{\max}^2)$. Moreover, as the principal curvatures are uniformly bounded and $d_X(x)=O(d_{\mathcal{H}}(X,\mathcal{T}))$, we get

$$\det(D_{\restriction_A}\pi_X)(x) = (1+O(\alpha_{\max}^2))(1+O(d_{\mathcal{H}}(X,\mathcal{T}))) = 1+O(\alpha_{\max}^2+d_{\mathcal{H}}(X,\mathcal{T})) \tag{4.5}$$

as $\alpha_{\max}^2, d_{\mathcal{H}}(X,\mathcal{T})\to 0$. The proposition follows by changing the variable in the formula of the area. □

In view of Lemma 4.8 let us introduce the following set of Assumptions:

Hypothesis 2. Let $(\mathcal{T}_h)_h$ be a sequence of triangulations indexed by a parameter $h>0$ decreasing to 0 such that

(*i*) for any $h>0$, the triangulation $\mathcal{T}_h$ is h-admissible for X;

(ii) the sequence $\alpha^h_{\max} = O(h)$ where $\alpha^h_{\max}$ is the angle of Definition 4.7 for the triangulation $\mathcal{T}_h$.

Remark 4.9. The parameter $h > 0$ is both the index of the triangulation and a measure of the precision of the triangulation. The idea is to consider decreasing h yielding to a more and more accurate.

This implies in particular the following result:

Proposition 4.10 (Convergence of the area). Let X be a surface satisfying Hypothesis 1 and $(\mathcal{T}_h)_h$ a sequence of triangulation satisfying Hypothesis 2. Then we have $\lim\limits_{h\to 0} \mathcal{H}^2(\mathcal{T}_h) = \mathcal{H}^2(X)$.

Proof. The proof follows from Lemma 4.8 and (iv) of Definition 4.4. □

Proposition 4.10 is a generalization of Corollary 5 of [19] to surfaces with smooth boundaries.

4.3 From the triangulation to the surface

In this section we define how to carry a signal from the triangulation to the surface.

Definition 4.11 (Projection). For every function f defined on an admissible triangulation for X we define the projection of f onto X by

$$f^\ell : X \to \mathbb{R}\,, \qquad f^\ell(\pi_X(x)) = f(x) \qquad x \in \mathcal{T}^{\text{in}}\,.$$

We point out that the function f^ℓ carries on X the signal defined on $\mathcal{T}^{\text{in}}$.

Proposition 4.12. Let $h > 0$ and $\mathcal{T}$ be and an admissible h-triangulation for X. Then, for every $f \in W^{1,\infty}(\mathcal{T},\mathbb{R})$, we have

$$\begin{aligned} \|f^\ell\|_{L^p(X)} &= \|f\|_{L^p(\mathcal{T}^{\text{in}})} + O(\alpha^2_{\max} + d_{\mathcal{H}}(X,\mathcal{T})), \\ \|\nabla^X f^\ell\|_{L^p(X)} &= \|\nabla^{\mathcal{T}^{\text{in}}} f\|_{L^p(\mathcal{T}^{\text{in}})} + O(\alpha^2_{\max} + d_{\mathcal{H}}(X,\mathcal{T})). \end{aligned}$$

for every $p \in [1,\infty]$, as $\alpha^2_{\max}, d_{\mathcal{H}}(X,\mathcal{T}) \to 0$.

Proof. The first equality is proved by performing the change of variables $y = \pi_X(x)$ and using Lemma 4.8. The second relationship is proved by applying the chain rule. A rigorous proof is given in [11] Lemma 3. □

5 Discretization

5.1 Notations

Let $\mathcal{T}$ be a triangulation in the sens of Definition 4.1. We denote by N_v, N_e, and N_t the number of vertices, edges, and triangles of $\mathcal{T}$ respectively. The family $\{v_i\}_{i=1,\ldots,N_v}$ denotes the vertices of the triangulation.

For every $k = 1,\ldots,N_t$, we denote by $\{v^k_i\}_{i=1,2,3}$ the vertices of the triangle $T_k \in \mathcal{T}$, $\left\{v^k_{ij}\right\}_{1\leqslant i<j\leqslant 3}$ the center of the edge linking v^k_i to v^k_j, and $v^k_0 \doteq \frac{1}{3}\sum_{i=1}^3 v^k_i$ the center of mass of the triangle (see Figure 6). Analogously we denote by $\{f^k_i\}_{0\leqslant i\leqslant 3}$ the values of the function f at location $\{v^k_i\}_{0\leqslant i\leqslant 3}$ of T_k.

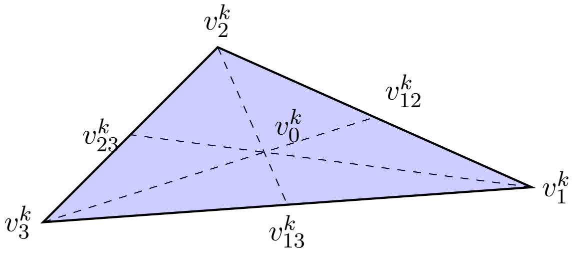

Figure 6: Labels of various points in the triangle T_k.

5.2 P_0 and P_1 triangular finite elements

Let us start with the following definition,

Definition 5.1. For a given triangulation $\mathcal{T}$, we denote by $\mathbb{P}_0(\mathcal{T})$ (resp. $\mathbb{P}_1(\mathcal{T})$), the set of functions that are constant on the interior of each triangle and null on their sides (resp. the set of the continuous functions that are affine on each triangle).

The elements of $\mathbb{P}_0(\mathcal{T})$ (resp. $\mathbb{P}_1(\mathcal{T})$) are completely described by their values $(f_0^k)_k$ at the center of mass $(v_0^k)_k$ (resp. their values $(\{f_i^k\}_{1\leqslant i\leqslant 3})_k$ at vertices $(\{v_i^k\}_{1\leqslant i\leqslant 3})_k$) of the triangulation. Note that for $f \in \mathbb{P}_1(\mathcal{T})$, and each triangle $T_k \in \mathcal{T}$

$$\forall\, f \in \mathbb{P}_1(\mathcal{T})\,, \quad f_0^k = f(v_0^k) = f(\sum_{i=1}^{3} v_i^k/3) = \sum_{i=1}^{3} f(v_i^k)/3 = \sum_{i=1}^{3} f_i^k/3\,.$$

On the other hand, if $f \in \mathbb{P}_0(\mathcal{T})$, as f is null on the sides of each triangle, we can not calculate f_0^k by the values at the vertices, and we can only set

$$\forall\, f \in \mathbb{P}_0(\mathcal{T})\,, \quad f_0^k = f(v_0^k)\,.$$

We denote by p_0 the L^2-projection of $\mathbb{P}_1(\mathcal{T})$ on $\mathbb{P}_0(\mathcal{T})$ where for $f \in \mathbb{P}_1(\mathcal{T})$, the function $p_0(f)$ is the unique element of $\mathbb{P}_0(\mathcal{T})$ such that

$$p_0(f)(v_0^k) = f(v_0^k)\,, \tag{5.1}$$

i.e. the operator p_0 replace the affine approximation of a signal on each triangle by a constant approximation using the value at the center of mass.

A basis for $\mathbb{P}_1(\mathcal{T})$ is given by the family $\{\varphi\}_{i=1,\cdots,N_v}$ with $\varphi_i \in \mathbb{P}_1(\mathcal{T})$ and $\varphi_i(v_j) = \delta_{ij}$ (Kronecker's delta), for every $i = 1, \cdots, N_v$. Then, every $f \in \mathbb{P}_1(\mathcal{T})$ can be written as

$$\forall x \in \mathcal{T} \qquad f(x) = \sum_{j=1}^{N_v} f_j \varphi_j(x)\,, \quad f_j = f(v_j)\,.$$

Remark that there exists a bijection between $\mathbb{P}_1(\mathcal{T})$ and $\mathbb{R}^{N_v}$, defined by the following operator

$$P_1 \ : (f_1, \ldots, f_{N_v}) \in \mathbb{R}^{N_v} \quad \mapsto \quad f = \sum_{j=1}^{N_v} f_j\, \varphi_j \in \mathbb{P}_1(\mathcal{T}) \tag{5.2}$$

5.3 Discrete operators

For every $k = 1, \cdots, N_t$ the area of the triangle T_k is denoted by $|T_k|$ and is equal to $\frac{1}{2}\|\boldsymbol{n}_{T_k}\|$ where $\boldsymbol{n}_{T_k} = (v_2^k - v_1^k) \wedge (v_3^k - v_1^k)$.

5.3.1 Discrete norms on signal

Depending on how the continuous signal is discretized, various methods may be used to compute the norm of the discrete signal.

Formula exact on P_0-finite elements Let $p \geqslant 1$ and $f : \mathcal{T} \to \mathbb{R}$ a function in $L^p(\mathcal{T}, \mathbb{R})$. The p-power of the discrete L^p-norm of f is simply defined as

$$L_0^p[f, \mathcal{T}] \doteq \sum_{k=1}^{N_t} |T_k||f_0^k|^p. \tag{5.3}$$

Formula (5.3) is exact for signals that are (almost everywhere) constant on each triangle, *i.e.* we have $L_0^p[f, \mathcal{T}] = \|f\|_{L^p(\mathcal{T})}^p$ for any $f \in \mathbb{P}_0(\mathcal{T})$. If f is in $\mathbb{P}_1(\mathcal{T})$, then we have $L_0^p[f, \mathcal{T}] = \|p_0(f)\|_{L^p(\mathcal{T})}^p$.

Formula exact on P_1 finite elements In work, we need to compute L^p norms with $p = 1, 2$. Thence, if we consider a signal $f \in \mathbb{P}_1(\mathcal{T})$, it is sufficient to use a formula exact on piecewise quadratic polynomial to fit our needs. For instance the Newton-Cotes formula for triangular mesh (see [2] pages 178–179) is

$$L_1^p[f, \mathcal{T}] = \frac{1}{3} \sum_{k=1}^{N_t} |T_k|(|f_{12}^k|^p + |f_{13}^k|^p + |f_{23}^k|^p). \tag{5.4}$$

where for a piecewise linear signal $f \in \mathbb{P}_1(\mathcal{T})$ we have $f_{ij}^k \doteq \frac{1}{2}(f_i^k + f_j^k)$ for any $k = 1, \dots, N_t$ and $1 \leqslant i < j \leqslant 3$.

The formula (5.4) is exact if $p = 2$ (*i.e.* $L_1^2[f, \mathcal{T}] = \|f\|_{L^2(\mathcal{T})}^2$) since the function ${f^2}_{\restriction T_k}$ is a polynomial of degree 2 for any $k = 1, \dots, N_t$. The formula (5.4) is also exact if $p = 1$ and f has constant sign on each triangle (*i.e.* we have $L_1^1[f, \mathcal{T}] = \|f\|_{L^1(\mathcal{T})}$ if $f \geqslant 0$ or $f \leqslant 0$). If the signal $f \in \mathbb{P}_1(\mathcal{T})$ has a changing sign on a given triangle T_k, we briefly explain how the quantity $L_1^1[f_{\restriction T_k}, \{T_k\}]$ is computed in practice. First, remark that at least two of the f_i^k's have to be of the same sign. Without lost of generality, assume that$f_1^k < 0$ and $f_2^k > 0$, $f_3^k \geqslant 0$ (as in Figure 7). As f is linear on T_k, we can easily compute the coordinates of the points v_4^k, v_5^k belonging to the edges of T_k and satisfying

$$f(tv_4^k + (1-t)v_5^k) = 0, \text{for } t \in [0, 1].$$

The triangle T_k can be split in three subtriangles $T_{k_1}, T_{k_2}, T_{k_3}$ with vertices (v_1^k, v_4^k, v_5^k), (v_2^k, v_5^k, v_4^k), (v_2^k, v_3^k, v_5^k) and with corresponding signals $P_1(f_1^k, 0, 0)$, $P_1(f_2^k, 0, 0)$, $P_1(f_2^k, f_3^k, 0)$ respectively (the bijection $P_1 : \mathbb{R}^3 \to \{T_k\}$ is defined by (5.2)). Thence, the exact L^1 norm of $f_{\restriction T_k} \in \mathbb{P}_1(\{T_k\})$ may now be computed by applying the Newton-Cotes formula on this three subtriangles:

$$L_1^1[f_{\restriction T_k}, \{T_k\}] = \frac{1}{3} \sum_{i=1}^{3} |T_{k_i}|(|f_{12}^{k_i}| + |f_{13}^{k_i}| + |f_{23}^{k_i}|).$$

The general case follows as $L_1^1[f, \mathcal{T}] = \sum_{k=1}^{N_t} L_1^1[f_{\restriction T_k}, \{T_k\}]$.

5.3.2 Discrete norm on signal derivative

Let assume that $f \in \mathbb{P}_1(\mathcal{T})$. We give in the following the discrete operators needed to compute the discrete H^1 and BV norms. For every $T_k \in \mathcal{T}$ and for every $f \in \mathbb{P}_1(\mathcal{T})$, the gradient of f on T_k

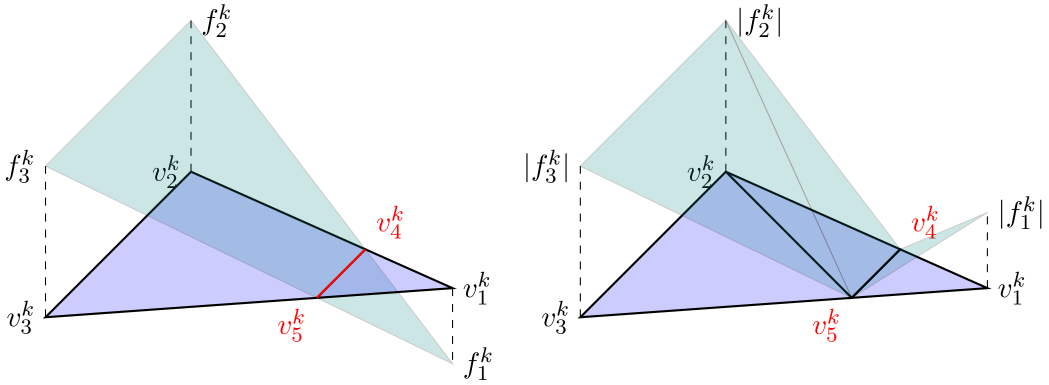

Figure 7: The L^1 norm on a triangle T_k of a piecewise linear signal (f_1^k, f_2^k, f_3^k) is the non-oriented volume between the blue and green triangles. This figure illustrates how T_k is divided in 3 subtriangles to compute of the L^1 norm of a signal.

can be computed by

$$[\nabla_{\mathcal{T}} f]_{T_k} = \frac{e_2^k \wedge e_3^k}{\|e_2^k \wedge e_3^k\|^2} \wedge \left(f_1^k e_1^k + f_2^k e_2^k + f_3^k e_3^k\right) \tag{5.5}$$

where

$$e_1^k = v_3^k - v_2^k\,, \quad e_2^k = v_1^k - v_3^k\,, \quad e_3^k = v_2^k - v_1^k\,.$$

In this framework, gradient $\nabla_{\mathcal{T}} f$ is constant on each triangle and by convention is null on the edges.

Total variation. The total variation of $f \in \mathbb{P}_1$ on $\mathcal{T}$ is given by

$$V[f, \mathcal{T}] = \sum_{k=1}^{N_t} |T_k| \|[\nabla_{\mathcal{T}} f]_{T_k}\|\,. \tag{5.6}$$

H^1-norm. For $f \in \mathbb{P}_1(\mathcal{T})$, the square of the L^2-norm of the gradient is given by

$$H[f, \mathcal{T}] = \sum_{k=1}^{N_t} |T_k| \|[\nabla_{\mathcal{T}} f]_{T_k}\|^2\,. \tag{5.7}$$

Remark that $H[f, \mathcal{T}] = L_0^2[\|\nabla_{\mathcal{T}} f\|, \mathcal{T}]$ as $f \in \mathbb{P}_1$ and by formula (5.5) we have $\|\nabla_{\mathcal{T}} f\| \in \mathbb{P}_0(\mathcal{T})$.

5.3.3 The fvarifold norm

The fvarifold associated with the discrete fshape $(\mathcal{T}, f)$ is naturally defined by $\mu_{(\mathcal{T},f)}$. However, in order to simplify the computation we approximate such a fvarifold by a discrete measure $\boldsymbol{\mu}_{(\mathcal{T},f)}$. Such an approximation is set in the same way in the P_0 and P_1-finite elements setting.

The discrete fvarivold norm is defined as

$$\boldsymbol{\mu}_{(\mathcal{T},f)} \doteq \sum_{k=1}^{N_t} |T_k| \delta_{(v_0^k, V_k, f_0^k)} \tag{5.8}$$

where

$$v_0^k = \frac{1}{3}(v_1^k + v_2^k + v_3^k),\ \ f_0^k = f(v_0^k),\ \ V_k \doteq \mathrm{Span}\{v_2^k - v_1^k, v_3^k - v_1^k\}\,.$$

The discrete fvarifold-norm is defined by

$$\mathrm{Var}[\mu_{(\mathcal{T},f)}] \doteq \|\boldsymbol{\mu}_{(\mathcal{T},f)}\|^2_{W'} \tag{5.9}$$

which can be easily computed by (2.3). We point out that by formula (5.1) we have

$$\boldsymbol{\mu}_{(\mathcal{T},f)} = \boldsymbol{\mu}_{(\mathcal{T},p_0(f))} \qquad \forall\, f \in \mathbb{P}_1(\mathcal{T})\,.$$

Finally, as we identify the tangent space with the normal one, accordingly to (2.1), we define the discrete RKHS by the following kernels

$$k_e(v,v') = e^{-\frac{|v-v'|^2}{\sigma_e^2}}\,,\; k_t(V,V') = e^{-\frac{2(1-\langle \boldsymbol{n}_V, \boldsymbol{n}_{V'}\rangle^2)}{\sigma_t^2}}\,,\; k_f(s,s') = e^{-\frac{|s-s'|^2}{\sigma_f^2}}\,,$$

where $\boldsymbol{n}_V$ denotes a unit normal vector to V.

6 Discrete problems and Γ-convergence results

We now come back to the continuous "functional" matching problem defined by formula (3.1). The aim of this section is to show the Γ-convergence of well chosen discretized versions of these problems to their continuous counterpart. To this end, we have to compare functionals defined on different spaces. This can be done by projecting the discrete functional on the limit surface as described in Definition 4.11. Following [14], this leads to define a suitable topology (called in the following S-topology) in order to set a definition of Γ-convergence.

6.1 Discretization procedure

First of all, we discuss how to discretize (on an admissible triangulation) a signal defined on a surface. Let X be a surface verifying Hypothesis 1 and $\mathcal{T}$ be a h-admissible triangulation for X for some $h > 0$. We denote by f a signal on X belonging to $L^2(X)$ (resp. $H^1(X)$ or $BV(X)$). The aim of this Section is to define from f a P_0 or P_1 finite element f_h on $\mathcal{T}$.

According to property (*ii*) of Definition 4.4, by using the map Ext defined in (9.13), we can extend the manifold X to a larger suitable manifold $X^{+\eta}$ such that $\mathcal{T} \subset \mathcal{N}_h(X^{+\eta})$. Moreover, because of Theorem 9.5, the signal f can be extended to a signal $\tilde{f}$ defined on $X^{+\eta}$ which is $L^2(X^{+\eta})$ (resp. $H^1(X^{+\eta})$ and $BV(X^{+\eta})$) and with a small norm on $X^{+\eta} \setminus X$.

Let T be a triangle belonging to $\Delta_{\mathcal{T}}$. Depending on the regularity of f we consider two discretization procedure:

- the P_1-element: the piecewise linear f_h corresponding to f on T is defined as

  $$f_h = P_1(\tilde{f}(\pi_{X^{+\eta}}(v_1)), \tilde{f}(\pi_{X^{+\eta}}(v_2)), \tilde{f}(\pi_{X^{+\eta}}(v_3)))$$

  where v_1, v_2, v_3 denote the three vertices of T and P_1 is defined by (5.2).

- the P_0-element: as every P_0-element is null on each side of T, we define the piecewise (ae) constant f_h corresponding to f on T as

  $$f_h = \begin{cases} 0 & \text{on the sides of } T\,, \\ \frac{1}{3}\left(\tilde{f}(\pi_{X^{+\eta}}(v_1)) + \tilde{f}(\pi_{X^{+\eta}}(v_2)) + \tilde{f}(\pi_{X^{+\eta}}(v_3))\right) & \text{otherwise.} \end{cases}$$

  where v_1, v_2, v_3 denote the three vertices of T.

6.2 Preliminary result

In this section we prove a technical result that is useful in the following.

Lemma 6.1. Let X be a surface verifying Hypothesis 1 and $\mathcal{T}$ a h-admissible triangulation for X verifying Hypothesis 2. Then we have

$$\sup_{f\in\mathbb{P}_0(\mathcal{T})} \|\boldsymbol{\mu}_{(\mathcal{T},f)} - \mu_{(X,f^\ell)}\|_{W'} = O(h)\,, \tag{6.1}$$

and

$$\forall\, f \in \mathbb{P}_1(\mathcal{T}) \quad \|\boldsymbol{\mu}_{(\mathcal{T},f)} - \mu_{(X,f^\ell)}\|_{W'} = O(h)(1+\|\nabla f\|_{L^1(\mathcal{T})})\,. \tag{6.2}$$

Proof. Let $f\in\mathbb{P}_0(\mathcal{T})$. By the change of variables $x=\pi_X(y)$, because of Hypothesis 2 and formula (4.5), we have uniformly in $f\in\mathbb{P}_0(\mathcal{T})$ and $\varphi\in C_0^1(\mathbb{R}^3\times G(3,2)\times\mathbb{R})$,

$$\left|\int_X \varphi(x,T_xX,f^\ell(x))d\mathcal{H}^2(x) - \int_{\mathcal{T}^{\text{in}}}\varphi(y,T_y\mathcal{T}^{\text{in}},f(y))d\mathcal{H}^2(y)\right| \leqslant \|\varphi\|_{L^\infty(\mathbb{R}^3\times G(3,2)\times\mathbb{R})}\,O(h)\,.$$

Moreover, because of property (iv) in Definition 4.4, $\mu_{(\mathcal{T}^{\text{out}},f)}$ converges towards the null varifold as $h\to 0$. Then

$$\left|\int \varphi d(\mu_{(\mathcal{T},f)} - \mu_{(X,f^\ell)})\right| \leqslant \|\varphi\|_{L^\infty(\mathbb{R}^3\times G(3,2)\times\mathbb{R})}O(h)\,.$$

Now, if $f\in\mathbb{P}_0(\mathcal{T})$, then $f=f_0^k$ on the interior of every triangle T_k. Then, for every $\varphi\in C_0^1(\mathbb{R}^3\times G(3,2)\times\mathbb{R})$, we get

$$\begin{aligned}
|(\mu_{(\mathcal{T},f)} - \boldsymbol{\mu}_{(\mathcal{T},f)})(\varphi)| &\leqslant \sum_{k=1}^{N_t}\int_{T_k}|\varphi(x,T_x\mathcal{T},f(x)) - \varphi(v_0^k,V_k,f_0^k)|\,d\mathcal{H}^2(x)\\
&\leqslant \sum_{k=1}^{N_t}\|\varphi\|_{C^1(\mathbb{R}^3\times G(3,2)\times\mathbb{R})}\int_{T_k}\|(x,V_k,f(x)) - (v_0^k,V_k,f_0^k)\|_{\mathbb{R}^3\times G(3,2)\times\mathbb{R}}\,d\mathcal{H}^2(x)\\
&\leqslant \sum_{k=1}^{N_t}|T_k|\|\varphi\|_{C^1(\mathbb{R}^3\times G(3,2)\times\mathbb{R})}\text{diam}(T_k) \leqslant \mathcal{H}^2(\mathcal{T}_h)\|\varphi\|_{C^1(\mathbb{R}^3\times G(3,2)\times\mathbb{R})}O(h)\,.
\end{aligned}$$

where N_t denotes the number of triangles belonging to $\mathcal{T}$. So, by taking the supremum on the unit ball of $C_0^1(\mathbb{R}^3\times G(3,2)\times\mathbb{R})$ and by using (2.2), we get

$$\|\mu_{(\mathcal{T},f)} - \boldsymbol{\mu}_{(\mathcal{T},f)}\|_{W'} \leqslant C\|\mu_{(\mathcal{T},f)} - \boldsymbol{\mu}_{(\mathcal{T},f)}\|_{(C_0^1(\mathbb{R}^3\times G(3,2)\times\mathbb{R}))'} \leqslant O(h)\mathcal{H}^2(\mathcal{T})\,.$$

Then, we have $\|\mu_{(X,f^\ell)} - \boldsymbol{\mu}_{(\mathcal{T},f)}\|_{W'}\leqslant O(h)$ which proves (6.1).

If $f\in\mathbb{P}_1(\mathcal{T})$ the proof is similar, but the bound of $|(\mu_{(\mathcal{T},f)} - \boldsymbol{\mu}_{(\mathcal{T},f)})(\varphi)|$ depends on f because

$$\forall\, x\in T_k \quad |f(x) - f_0^k| \leqslant \|\nabla f\|_{L^1(T_k)}\text{diam}(T_k)$$

so that, by the same arguments, we get

$$\|\boldsymbol{\mu}_{(\mathcal{T},f)} - \mu_{(X,f^\ell)}\|_{W'} \leqslant O(h)(1+\|\nabla f\|_{L^1(\mathcal{T})})\,.$$

which proves (6.2)

□

6.3 The L^2-model

We prove a Γ-convergence result for the discretization of the problem (3.2). The proof is given in the relaxed setting of measures defined in Definition 3.3. We refer to Section 3.1 for the main notations. Let $\{\mathcal{T}_h\}$ be a sequence of h-admissible triangulations for X verifying Hypothesis 2. The discrete energy $E_h : \mathbb{P}_0(\mathcal{T}_h) \to \mathbb{R} \cup \{+\infty\}$ is defined by

$$E_h(f_h) \doteq \frac{\gamma_f}{2} L_0^2[f_h, \mathcal{T}_h] + \frac{\gamma_W}{2} \mathrm{Var}[\mu_{(\mathcal{T}_h, f_h)} - \mu_{(\mathcal{Y}_h, g_h)}] \tag{6.3}$$

where $\mathcal{Y}_h$ is a h-admissible triangulation for Y verifying Hypothesis 2 and $g_h \in \mathbb{P}_0(\mathcal{Y}_h)$ is the discrete signal on $\mathcal{Y}_h$ obtained by applying the discretization procedure described in Section 6.1 to g. We have in particular

$$\|\mu_{(Y,g)} - \boldsymbol{\mu}_{(\mathcal{Y}_h, g_h)}\|_{W'}^2 \to 0 \text{ as } h \to 0$$

We define also (for every h) the following discrete problem

$$\inf_{f_h \in \mathbb{P}_0(\mathcal{T}_h)} E_h(f_h). \tag{6.4}$$

We also suppose that γ_f/γ_W is independant from h and verifies the hypothesis of Theorem 3.2 for every h. An existence result for the discrete problem can be proved easily in the discrete setting.

Proposition 6.2. For every $h > 0$, there exists at least a solution to problem (6.4).

Proof. Simply notice that E_h is continuous in f_h, that $L_0^2[f_h, \mathcal{T}_h] = \sum_{k=1}^{N_t^h} |T_k||f_h(v_0^k)|^2$ is a coercive bilinear form on $\mathbb{P}_0(\mathcal{T}_h)$ and that $\mathrm{Var}[\mu_{(\mathcal{T}_h, f_h)} - \mu_{(\mathcal{Y}_h, g_h)}] = \|\boldsymbol{\mu}_{(\mathcal{T}_h, f_h)} - \boldsymbol{\mu}_{(\mathcal{Y}_h, g_h)}\|_{W'}^2$ is bounded. □

As the discrete and continuous functionals are not defined on the same space, we consider first the S-topology to compare the signals. We then define the Γ-convergence (see *e.g.*[14]) for the functional:

Definition 6.3 (S-topology and Γ-convergence). Let X be a surface satisfying Hypothesis 1. Let $(\mathcal{T}_h)_h$ be a sequence of h-admissible triangulations for X verifying Hypothesis 2 and f a function defined on X. In this definition, $(f_h)_h$ denotes a sequence of functions such that $f_h \in \mathbb{P}_0(\mathcal{T}_h)$ for every $h > 0$.

- We say that $(f_h)_h$ converges to f with respect to the S-topology ($f_h \overset{S}{\rightharpoonup} f$) if and only if

  $$\mu_{(X, f_h^\ell)} \overset{*}{\rightharpoonup} \mu_{(X,f)} \text{ in } \mathcal{M}^X , \tag{6.5}$$

  where for any $h > 0$, f_h^ℓ is the projection of f_h onto X (see Definition 4.11). This defines a generalized convergence between functions with different supports which is used to defines the Γ-convergence.

- We say that $(E_h)_h$ Γ-converges to E if:

  (i) **Lower bound:** for every $f \in L^2(X)$ and for every sequence $(f_h)_h$ such that $f_h \overset{S}{\rightharpoonup} f$, we have

  $$E(f) \leqslant \liminf_{h \to 0} E_h(f_h) ;$$

(*ii*) **Upper bound:** for every $f \in L^2(X)$ there exists a sequence $(f_h)_h$ such that $f_h \overset{S}{\rightharpoonup} f$, and

$$E(f) \geqslant \limsup_{h\to 0} E_h(f_h)\,.$$

Theorem 6.4. The sequence $(E_h)_h$ Γ-converges to the functional E defined in (3.2) with respect to the S-topology.

Proof. **Lower bound**. Let $(f_h)_h$ be a sequence of functions such that $f_h \in \mathbb{P}_0(\mathcal{T}_h)$ for every h and $f_h \overset{S}{\rightharpoonup} f \in L^2(X)$. As the functional $\tilde{E}$ defined in (3.4) is lower-semicontinuous with respect to the weak convergence of measures, we obtain

$$E(f) \;=\; \tilde{E}(\mu_{(X,f)}) \;\leqslant\; \liminf_{h\to 0} \tilde{E}(\mu_{(X,f_h^\ell)})\,. \tag{6.6}$$

Now, by change of variables and because of (2) and (4.5) we get

$$L_0^2[f_h,\mathcal{T}_h] = \|f_h\|^2_{L^2(\mathcal{T}_h)} \geqslant \|f_h\|^2_{L^2(\mathcal{T}_h^{\mathrm{in}})} \geqslant (1+O(h))\|f_h^\ell\|^2_{L^2(X)}\,. \tag{6.7}$$

Moreover, from Lemma 6.1, we have

$$\mathrm{Var}[\mu_{(\mathcal{T}_h,f_h)} - \mu_{(\mathcal{Y}_h,g_h)}] = \|\boldsymbol{\mu}_{(\mathcal{T}_h,f_h)} - \boldsymbol{\mu}_{(\mathcal{Y}_h,g_h)}\|^2_{W'} = \|\mu_{(X,f_h^\ell)} - \mu_{(Y,g_h^\ell)}\|^2_{W'} + O(h)\,. \tag{6.8}$$

Finally, by (6.7) and (6.8) and since $\|\mu_{(Y,g)} - \boldsymbol{\mu}_{(\mathcal{Y}_h,g_h)}\|_{W'} = o(1)$

$$E_h(f_h) \geqslant (1+O(h))E(f_h^\ell) + o(1) \geqslant (1+O(h))\tilde{E}(\mu_{(X,f_h^\ell)}) + o(1) \tag{6.9}$$

and, because of (6.6), this proves the lower bound condition.

Upper bound. As $C^1(X)$ is dense in $L^2(X)$ we can suppose that f is smooth (see Remark 9.6). We can then conclude by a diagonal extraction argument (see below).

For every sequence $(\mathcal{T}_h)_h$ of h-admissible triangulations for X verifying Hypothesis 2 we can define the functions $f_h \in \mathbb{P}_0(\mathcal{T}_h)$ defined on $\mathcal{T}_h$ by the Discretization Procedure of Section 6.1 for the setting of the P_0-finite elements. Then, we define a sequence $f_h \in L^\infty(\mathcal{T}_h)$ such that $\sup_h \|f_h\|_{L^\infty(\mathcal{T}_h)} \leqslant \|f\|_{L^\infty(X)}$. Thus, because of (*iv*) Definition 4.4, we obtain

$$\|f_h\|_{L^2(\mathcal{T}_h^{\mathrm{out}})} = O(h)\,. \tag{6.10}$$

Now, we get $f_h^\ell \to f$ strongly in $L^2(X)$, and, because of (5.3), Proposition 4.10, and Hypothesis 2, by change of variables, we obtain

$$\|f_h^\ell\|^2_{L^2(X)} = L_0^2[f_h,\mathcal{T}_h] + O(h)$$

so that

$$L_0^2[f_h,\mathcal{T}_h] \to \|f\|^2_{L^2(X)} \quad \text{as} \quad h\to 0\,.$$

In particular, (up to a subsequence) $f_h^\ell \to f$ a.e. which implies that $f_h \overset{S}{\rightharpoonup} f$ (meaning that $\mu_{(X,f_h^\ell)} \overset{*}{\rightharpoonup} \mu_{(X,f)}$) and, since Lemma 6.1 and Lemma 3.1, we also get

$$\mathrm{Var}[\mu_{(\mathcal{T}_h,f_h)} - \mu_{(\mathcal{Y}_h,g_h)}] = \|\boldsymbol{\mu}_{(\mathcal{T}_h,f_h)} - \boldsymbol{\mu}_{(\mathcal{Y}_h,g_h)}\|^2_{W'} \to \|\mu_{(X,f)} - \mu_{(Y,g)}\|^2_{W'}$$

Then, we have proved that $f_h \overset{S}{\rightharpoonup} f$, and

$$E(f) = \lim_{h\to 0} E_h(f_h).$$

Diagonal argument. Let $(f_n)_{n\in\mathbb{N}}$ be a sequence in $C^1(X)$ converging to $f \in L^2(X)$ in L^2 and pointwise. As the fvarifold-norm is continuous with respect to the pointwise convergence of the signal we have

$$\lim_{n\to+\infty} E(f_n) = E(f)\,.$$

Previous proof shows that, for every $n \in \mathbb{N}$ we can define a P_0-elements sequence f_n^i (formerly called f_h) such that

$$\forall\, n \in \mathbb{N}, \quad \lim_{i\to+\infty} E(f_n^i) = E(f_n)\,.$$

This means that

$$\forall \varepsilon > 0,\ \exists N(\varepsilon) \in \mathbb{N} : n \geqslant N \Rightarrow |E(f_n) - E(f)| < \varepsilon/2$$

and

$$\forall n \in \mathbb{N},\ \exists I(n) \in \mathbb{N} : i \geqslant I(n) \Rightarrow |E(f_n^i) - E(f_n)| < 1/n.$$

Let $\varepsilon > 0$, the sequence $(f_n^{I(n)})_{n\in\mathbb{N}}$ verifies

$$n \geqslant N(\varepsilon) \Rightarrow |E(f_n^{I(n)}) - E(f)| \leqslant |E(f_n^{I(n)}) - E(f_n)| + |E(f) - E(f_n)| \leqslant 1/n + \varepsilon/2$$

which yields to

$$\forall n \geqslant \max\{N(\varepsilon), 2/\varepsilon\} \Rightarrow |E(f_n^{I(n)}) - E(f)| \leqslant \varepsilon.$$

The last inequality is valid for arbitrarily small $\varepsilon > 0$ and it eventually proves that

$$\lim_{n\to+\infty} E(f_n^{I(n)}) = E(f)\,.$$

□

For the following result, we consider the assumptions of Theorem 3.2, that is that X is a C^p oriented connected compact 2 dimensional submanifold ($p \geqslant 2$), Y is a finite volume 2-rectifiable subset of $\mathbb{R}^3$ and that W is continuously embedded in $C_0^m(\mathbb{R}^3 \times G(3,2) \times \mathbb{R})$ with $m \geqslant p$.

Theorem 6.5 (Convergence of minima). Assume that hypothesis of Theorem 3.2 hold and that X satisfies Hypothesis 1. Let $(\mathcal{T}_h)_h$ be a sequence of admissible triangulations for X verifying Hypothesis 2. Then if γ_f/γ_W is large enough,

$$\lim_{h\to 0} \min_{f\in\mathbb{P}_0(\mathcal{T}_h)} E_h(f) = \min_{f\in L^2(X)} E(f).$$

Moreover, if (f_h) is a sequence of minimizers of the functionals E_h, then, up to the extraction of a subsequence, there exists $f_* \in C^{p-1}(X)$ such that $f_{h_k} \overset{S}{\rightharpoonup} f_*$ and $E(f_*) = \min_{f\in L^2(X)} E(f)$.

Proof. The inequality

$$\lim_{h\to 0} \min_{f\in\mathbb{P}_0(\mathcal{T}_h)} E_h(f) \leqslant \min_{f\in L^2(X)} E(f). \tag{6.11}$$

follows easily from the upper bound condition of Γ-convergence.

Let us look at the other inequality and consider $f_h \in \mathbb{P}_0(\mathcal{T}_h)$ be a minima of E_h for any $h > 0$. Because of Theorem 3.2 (in particular (3.3)) we have

$$\|f_h\|_{L^\infty(\mathcal{T}_h)} \leqslant C\frac{\gamma_W}{\gamma_f}(\mathcal{H}^2(\mathcal{T}_h) + \mathcal{H}^2(\mathcal{Y}_h))\,.$$

As the areas of the triangulations converge to the areas of the respective surfaces, we can assume that the sequence $(f_h^\ell)_\ell$ is uniformly bounded on X. It yields that the measures $\mu_{(X,f_h^\ell)}$ are supported on a compact set. Thence, the sequence $\{\mu_{(X,f_h^\ell)}\}$ is tight and, because of the Prokhorov's theorem, it weak-$*$ converges (up to a subsequence) to some $\mu_\infty \in \mathcal{M}^X$. Then, by using the lower semicontinuity of $\tilde{E}$ with respect to the weak-$*$ convergence of measures and the fact that $\tilde{E}$ is minimized by a L^2-function (see Section 3.1), we get

$$\min_{f\in L^2(X)} E(f) \leqslant \tilde{E}(\mu_\infty) \leqslant \liminf_{h\to 0} \tilde{E}(\mu_{(X,f_h^\ell)})\,.$$

Now, since (3.5) we have $\tilde{E}(\mu_{(X,f_h^\ell)}) = E(f_h^\ell)$ and in the same way we get (6.9) we have $(1+O(h))E(f_h^\ell) + o(1) \leqslant E_h(f_h)$. It yields,

$$\min_{f\in L^2(X)} E(f) \leqslant \tilde{E}(\mu_\infty) \leqslant \liminf_{h\to 0} \tilde{E}(\mu_{(X,f_h^\ell)}) \leqslant \liminf_{h\to 0} \min_{f\in \mathbb{P}_0(\mathcal{T}_h)} E_h(f)$$

that gives the needed inequality. Using (6.11), we get also that $\min_{f\in L^2(X)} E(f) = \tilde{E}(\mu_\infty)$, and from Theorem 3.2 that there exists $f_* \in C^{p-1}(X)$ such that $\mu_\infty = \mu_{(X,f_*)}$. Thus, $f_h \overset{S}{\rightharpoonup} f_*$.

□

6.4 The BV-model

We study in this section the Γ-convergence of the discretization of (3.7). The Sobolev case can be treated by the same arguments by considering the discretized H^1-norm instead of the BV-one (see Remark 6.10). In this section we suppose that $\{\mathcal{T}_h\}$ (resp. $\{\mathcal{Y}_h\}$) is a sequence of h-admissible triangulations of X (resp. Y) verifying Hypothesis 2 and belonging to $\mathbb{T}_C$ for some $C > 0$ (see Definition 4.2). Then, for every h, we define the dicrete energy $E_h : \mathbb{P}_1(\mathcal{T}_h) \to \mathbb{R}\cup\{+\infty\}$ by

$$E_h(f_h) = \Big(L_1^1[f_h,\mathcal{T}_h] + V[f_h,\mathcal{T}_h]\Big) + \frac{\gamma_W}{2}\mathrm{Var}[\mu_{(\mathcal{T}_h,f_h)} - \mu_{(\mathcal{Y}_h,g_h)}] \tag{6.12}$$

where $g_h \in \mathbb{P}_1(\mathcal{Y}_h)$ is the discrete signal on $\mathcal{Y}_h$ obtained by applying the discretization procedure described in Section 6.1 to g. That defines (for every $h > 0$) the following discrete problem

$$\inf_{f_h\in\mathbb{P}_1(\mathcal{T}_h)} E_h(f_h). \tag{6.13}$$

Proposition 6.6. For every $h > 0$, there exists at least a solution to problem (6.13).

Proof. For every $f \in \mathbb{P}_1(\mathcal{T}_h)$ we have $\|\nabla_{\mathcal{T}_h} f\|_{L^1(\mathcal{T}_h)} = V[f,\mathcal{T}_h]$ and $L_1^1[f,\mathcal{T}_h] = \|f\|_{L^1(\mathcal{T}_h)}$. Then every minimizing sequence is bounded in BV so that it weak-$*$ converges in BV and a.e. (up to a subsequence). The result follows from Lemma 3.1, the lower semicontinuity of the total variation with respect to the weak-$*$ convergence.

□

As in Section 6.3, we introduce the S-topology needed to define the Γ-convergence for functionals:

Definition 6.7. [**S-topology and Γ-convergence**] Let X be a surface satisfying Hypothesis 1 and $C > 0$. Let $(\mathcal{T}_h)_h$ be a sequence in $\mathbb{T}_C$ of admissible triangulations for X verifying Hypothesis 2 and f be a function on X. In this definition, $(f_h)_h$ denotes a sequence of functions such that $f_h \in \mathbb{P}_1(\mathcal{T}_h)$ for every $h > 0$.

- We say that $(f_h)_h$ converges to f with respect to the S-topology ($f_h \overset{S}{\rightharpoonup} f$) if and only if

$$\lim_{h\to 0} \|f_h^\ell - f\|_{L^1(X)} \tag{6.14}$$

  where for any $h > 0$, f_h^ℓ is the projection of f_h onto X (see Definition 4.11).

- We say that $(E_h)_h$ Γ-converges to E if:

  (i) **Lower bound:** for every $f \in BV(X)$ and for every sequence $(f_h)_h$ such that $f_h \overset{S}{\rightharpoonup} f$, we have
$$E(f) \leqslant \liminf_{h\to 0} E_h(f_h)$$

  (ii) **Upper bound:** for every $f \in BV(X)$ there exists a sequence $(f_h)_h$ such that $f_h \overset{S}{\rightharpoonup} f$ and
$$E(f) \geqslant \limsup_{h\to 0} E_h(f_h)$$

Theorem 6.8. The sequence $(E_h)_h$ defined by formula (6.12) Γ-converges to E with respect to the S-topology of Definition 6.7.

Proof. **Lower bound**. Let $(f_h)_h$ be a sequence of functions such that $f_h \in \mathbb{P}_1(\mathcal{T}_h)$ for every $h > 0$ and $f_h \overset{S}{\rightharpoonup} f \in BV(X)$. Thus we have
$$f_h^\ell \xrightarrow{L^1(X)} f$$
where f_h^ℓ is the projection of f_h onto X (see Definition 4.11). Without loss of generality we can suppose that
$$\sup_{h>0} E_h(f_h) < \infty\,. \tag{6.15}$$
By Proposition 4.12, Hypothesis 2, and condition (iv) in Definition 4.4, we get

$$\|f_h\|_{BV(\mathcal{T}_h)} \geqslant (1 + O(h))\|f_h^\ell\|_{BV(X)}\,, \tag{6.16}$$

which implies
$$(1 + O(h))\|f_h^\ell\|_{BV(X)} \leqslant \|f_h\|_{BV(\mathcal{T}_h)} = L_1^1[f_h, \mathcal{T}_h] + V[f_h, \mathcal{T}_h]. \tag{6.17}$$

Moreover, by Lemma 6.1 and equation (6.15), we have

$$\|\boldsymbol{\mu}_{(\mathcal{T}_h,f_h)} - \mu_{(X,f_h^\ell)}\|_{W'}^2 \leqslant O(h)\,. \tag{6.18}$$

As $f_h^\ell \overset{L^1(X)}{\rightarrow} f$, we get that

$$\mathrm{Var}[\mu_{(\mathcal{T}_h,f_h)} - \mu_{(\mathcal{Y}_h,g_h)}] \to \|\mu_{(X,f)} - \mu_{(Y,g)}\|_{W'}^2\,. \tag{6.19}$$

Now, the BV-norm is lower semicontinuous with respect to the L^1-convergence then, because of (6.17) and (6.19), we get

$$E(f) \leqslant \liminf_{h\to 0} \left(\|f_h^\ell\|_{BV(X)} + \frac{\gamma_W}{2}\mathrm{Var}[\mu_{(\mathcal{T}_h,f_h)} - \mu_{(\mathcal{Y}_h,g_h)}]\right) \leqslant \liminf_{h\to 0} E_h(f_h). \tag{6.20}$$

Upper bound. As every function in $BV(X)$ can be approximated by a sequence of $C^1(X)$ functions with respect to the strict topology (see Theorem 9.5), we can assume that $f \in C^1(X)$.

The general case ensues by a diagonal extraction argument similar to the one given in the proof of Theorem 6.4.

Section 6.1, we detailed the way we can define $f_h \in \mathbb{P}_1(\mathcal{T}_h)$ for every h-admissible triangulations $\mathcal{T}_h$ for X. We remind that, in the discretization procedure, for every $h > 0$, we define an extension $X^{+\eta}$ of the manifold X and, afterwards, we extend f to a function $\tilde{f} \in BV(X^{+\eta})$ that is used to define f_h. Of course the extension $X^{+\eta}$ can depend on h, but in the following we prove some estimates for a fixed $h > 0$ and only write $X^{+\eta}$. In particular, we have

$$\|\tilde{f}\|_{W^{1,\infty}(X^{+\eta})} \leqslant \|f\|_{W^{1,\infty}(X)} \tag{6.21}$$

which implies that a $f_h \in W^{1,\infty}(\mathcal{T}_h)$ and $\sup_h \|f_h\|_{W^{1,\infty}(\mathcal{T}_h)} \leqslant \|f\|_{W^{1,\infty}(X)}$. This is essentially due to the extension procedure by symmetrization defined in Theorem 9.5.

Since Theorem 3.1.6 p. 124 in [9] (applied with $k = s = 0$, $p = \infty$, $m = q = 1$), we get

$$\|\tilde{f} \circ \pi_{X^{+\eta}} - f_h\|_{BV(\mathcal{T}_h)} = \|\tilde{f} \circ \pi_{X^{+\eta}} - f_h\|_{W^{1,1}(\mathcal{T}_h)} \leqslant Ch^2 \|\tilde{f} \circ \pi_{X^{+\eta}}\|_{W^{1,\infty}(\mathcal{T}_h)} \tag{6.22}$$

where $C > 0$ is a constant and $\tilde{f}$ is the extension of f on the extended manifold $X^{+\eta}$. More precisely, to obtain the previous estimate from Theorem 3.1.6 p. 124 in [9], we need to sum on all the triangles, use (4.2), and the fact that the area of every triangle is bounded by $\pi(h/2)^2$.

Now, because of *(iv)* Definition 4.4, we have

$$\|f_h\|_{BV(\mathcal{T}_h^{\text{out}})} = O(h)\,, \tag{6.23}$$

so that, by Proposition 4.12 and (6.21), we have

$$\|f - f_h^\ell\|_{BV(X)} = \|\tilde{f} \circ \pi_{X^{+\eta}} - f_h\|_{BV(\mathcal{T}_h^{\text{in}})} + O(h)\,,$$

$$\|\tilde{f} \circ \pi_{X^{+\eta}}\|_{W^{1,\infty}(\mathcal{T}_h)} \leqslant \|f\|_{W^{1,\infty}(X)} + O(h)$$

that, with (6.22), give

$$\|f - f_h^\ell\|_{BV(X)} = O(h)\,.$$

This proves in particular that $f_h^\ell \to f$ strongly in $L^1(X)$ (which means that $f_h \xrightarrow{S} f$) and the convergence of the total variation term, because

$$\|\nabla_X f_h^\ell\|_{L^1(X)} = \|\nabla_{\mathcal{T}_h} f_h\|_{L^1(\mathcal{T}_h^{\text{in}})} + O(h) = V[f_h, \mathcal{T}_h] + O(h)\,.$$

Moreover, Proposition 4.12 implies

$$\|f_h^\ell\|_{L^1(X)} = \|f_h\|_{L^1(\mathcal{T}_h)} = L_1^1[f_h, \mathcal{T}_h] + O(h),$$

so that

$$L_1^1[f_h, \mathcal{T}_h] \to \|f\|_{L^1(X)}^1 \quad \text{as} \quad h \to 0.$$

The convergence of the varifold term follows by Lemmas 6.1 and 3.1. Then

$$E(f) = \lim_{h \to 0} E_h(f_h).$$

□

Theorem 6.9 (Convergence of minima). Let $(\mathcal{T}_h)_h$ be a sequence of admissible triangulations for X verifying Hypothesis 2. Let $(f_h)_h$ be a sequence of minima of E_h (i.e., $E_h(f_h) = \min_{f \in \mathbb{P}_1(\mathcal{T}_h)} E_h(f)$). Then, $(f_h^\ell)_h$ weakly-$*$ converges in $BV(X)$ (up to a subsequence) to a minimum of E and

$$\lim_{h \to 0} \min_{f \in \mathbb{P}_1(\mathcal{T}_h)} E_h(f) = \min_{f \in BV(X)} E(f).$$

Proof. From the previous proposition we have that E_h Γ-converges to E. We consider the sequence $(f_h \in \mathbb{P}_1(\mathcal{T}_h))$ of the minima of E_h and, without loss of generality, we can also suppose that

$$\sup_{h>0} E_h(f_h) < \infty\,.$$

As for (6.17), we have

$$\|f_h^\ell\|_{BV(X)} \leqslant L_1^1[f_h, \mathcal{T}_h] + V[f_h, \mathcal{T}_h] + O(h),$$

so that $(f_h^\ell)_h$ is uniformly bounded in $BV(X)$. Then, there exists a subsequence (not relabeled) such that $(f_h^\ell)_h$ weak-$*$ converges to f^∞ in $BV(X)$ and, by Lemmas 6.1 and 3.1, we get

$$\mathrm{Var}_h[\mu_{(\mathcal{T}_h,f_h)} - \mu_{(\mathcal{Y}_h,g_h)}] \to \|\mu_{(X,f^\infty)} - \mu_{(Y,g)}\|_{W'}^2.$$

Then, similarly to (6.20), by lower semicontinuity, we get

$$\min_{f\in BV(X)} E(f) \leqslant E(f^\infty) \leqslant \lim_{h\to 0} \min_{f\in\mathbb{P}_1(\mathcal{T}_h)} E_h(f).$$

The other inequality follows from the upper bound condition of Γ-convergence. It follows in particular that f^∞ is a minimum of E. □

Remark 6.10. (**The Sobolev case**) The discrete problem for the H^1-model is defined in the same way by considering the discrete energy

$$E_h(f) = \frac{\gamma_f}{2}\left(L_1^2[f, \mathcal{T}_h] + H_h[f, \mathcal{T}_h]\right) + \frac{\gamma_W}{2}\mathrm{Var}_h[\mu_{(\mathcal{T}_h,f)} - \mu_{(\mathcal{Y}_h,g_h)}].$$

Then, Theorem 6.8 and Proposition 6.9 are still true in this case and their proofs can be straightforward generalized by considering as S-topology the L^2-convergence of the projection (i.e., $f_h \xrightarrow{S} f$ if $f_h^\ell \to f$ strongly in $L^2(X)$) and using the compactness with respect to the weak topology of H^1 (see Remark 3.6).

7 Numerical results

In this section we show some numerical results illustrating the effect of the different penalty terms based on L^2, H^1 or BV norms on the optimal solution. All the codes and data used in this examples are available at `https://github.com/fshapes/fshapesTk`.

The energy is discretized in the framework of the finite elements as detailed in Section 5 and 6.1. Note, that all the simulations are performed with a number P of points fixed. Moreover, in order to apply a gradient descent algorithm we choose to consider a smoothed version of discrete BV norm (the discrete L^2 and H^2 being differentiable). For the numeric simulations, we define the discrete operators (5.6) with the smoothed norm $\|\cdot\|_\varepsilon = \sqrt{(\cdot)^2 + \varepsilon^2}$ instead of the classic euclidean norm. This makes differentiable the L^1-norms and the evaluation of the jump part of the total variation, for every finite element. Note that such a smoothed energy Γ-converges to the initial one as ε goes to 0, and may justify such an approximation.

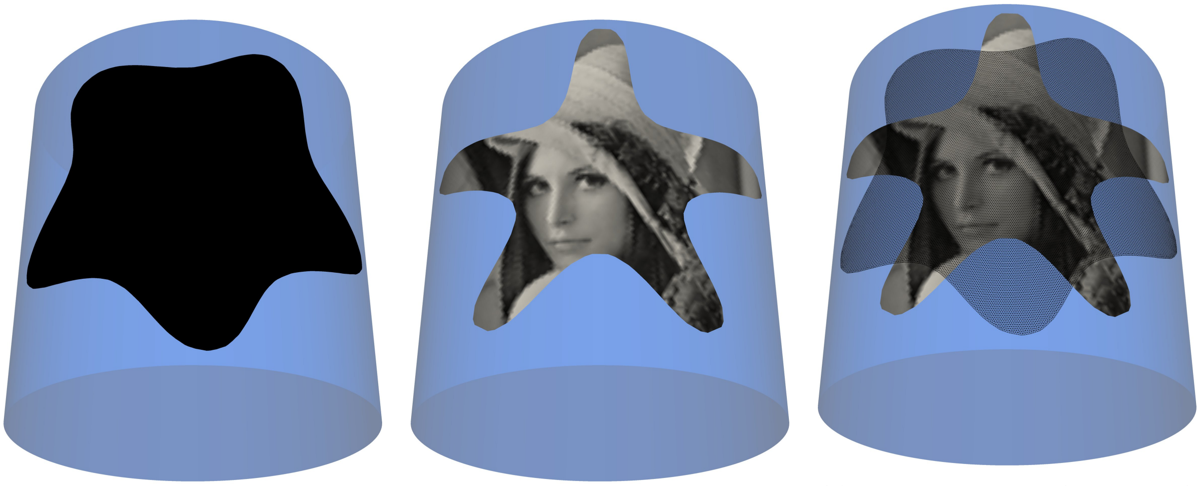
(a) Source $(X, 0)$

(b) Target (Y, g)

(c) Relative position (mesh view)

Figure 8: 8a: the initial fshape is a fat smooth star (same as Figure 1a). 8b: the target fshape (Y, g) is a thin star with Lena picture as grey level signal (black is 0 and white is 1). Compared to Figure 1b, the pixel effect on the target has disappeared because of the P_1 discretization (see Section 5). The blue cylinder is just drawn to help to see the perspective.

7.1 The melting smooth stars

We consider the matching problem between the two fshapes drawn in Figures 8a and 8b. These fshapes are the P_1 versions of the fshapes pictured Figure 1. Recall that we are interested in finding a signal f defined on X so that the fshape (X, f) is as close as possible to the target fshape (Y, g). The geometric support X remains fixed. As the L^2-model is given by Example 3.4, we show here only the effects of the BV and H^1 penalties.

We analyze in particular the impact of the volume and gradient term by considering the following weighted energies of the residual signal:

$$E(f) = pen(f) + \tfrac{1}{2}\|\mu_{(X,f)} - \mu_{(Y,g)}\|^2_{W'},$$

with

$$pen(f) = \begin{cases} \alpha\|f\|_{L^1(X)} + \beta|Df|(X), & BV \text{ model} \\ \alpha\|f\|^2_{L^2(X)} + \beta\|\nabla_X f\|^2_{L^2(X)}, & H^1 \text{ model} \end{cases}.$$

For sake of readability we have written the continuous version of the functional E but the minimization is obviously performed on the discrete version. The optimal fshape is defined by (X, f^*) where f^* is a (possibly local) minimum point (of the discrete version) of E found after an adaptive gradient descent.

In Figure 9 and 10 we show some simulations for different values of the parameters $\alpha > 0$ and $\beta > 0$. The main difference with Figure 2 is the absence of oscillations for the signal f^* in the non overlapping part of the source and target fshapes. Nevertheless, if β is chosen too small, oscillations may appeared as in Figure 10c.

7.2 The OCT dataset

We consider the two fshapes shown in Figure 11. These data are obtained by segmentation from volumetric images of the retina acquired by optical coherence tomography ([16, 17]). The

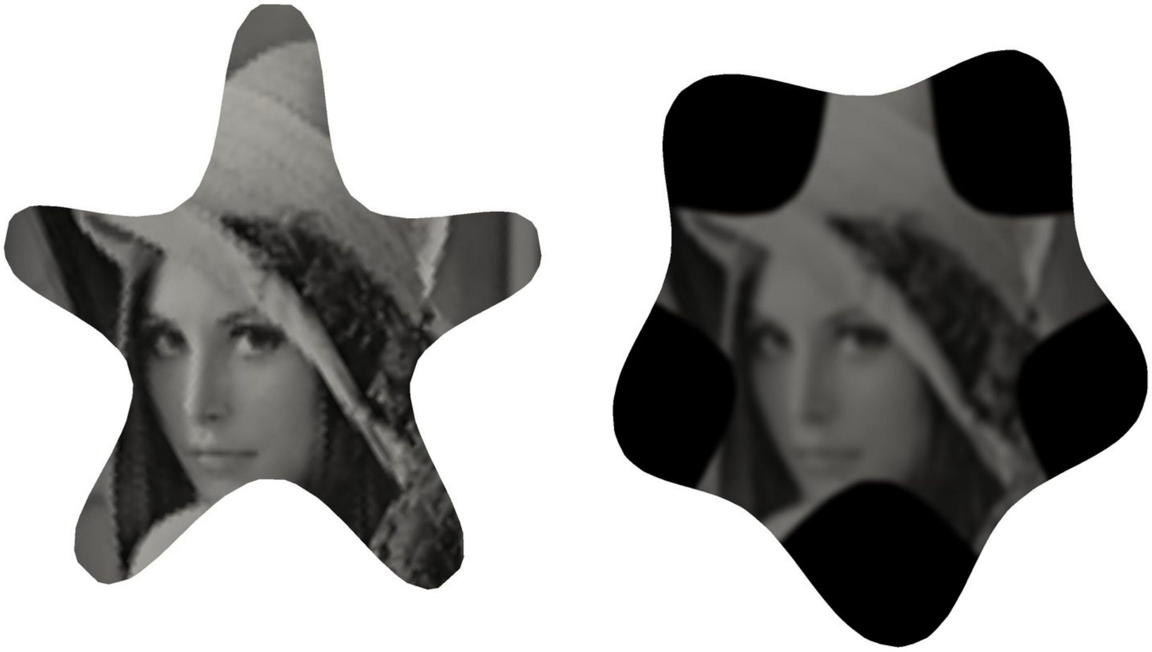

(a) The target (Y, g)

(b) $\alpha = 0.00125$ and $\beta = 0.125$.

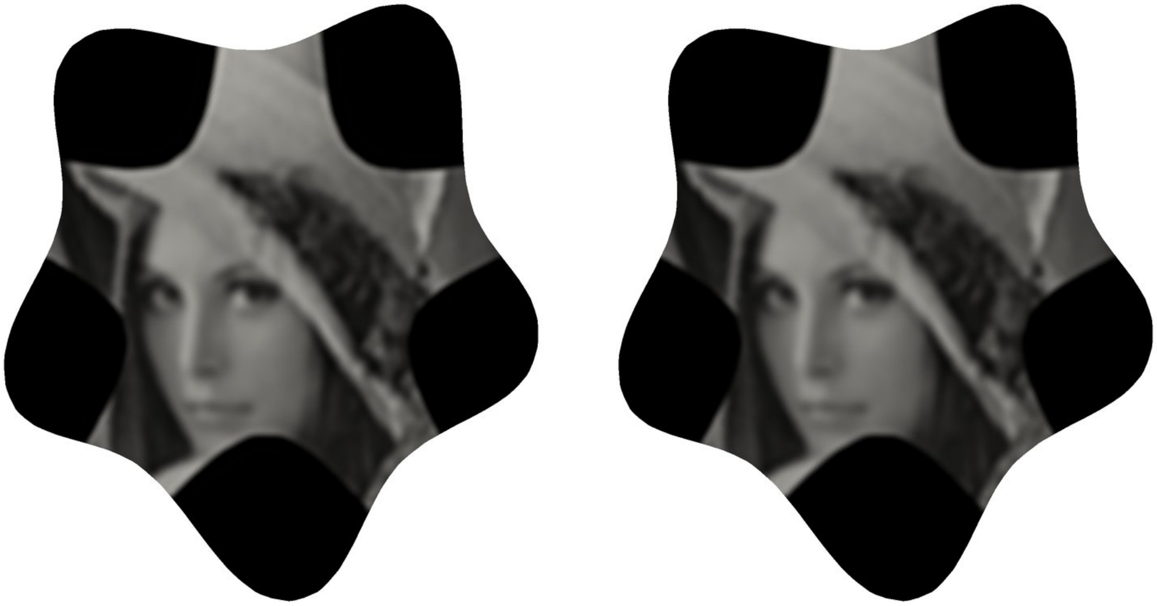

(c) $\alpha = 0.00125$ and $\beta = 0.0125$.

(d) $\alpha = 0.125$ and $\beta = 0.0125$.

Figure 9: Results for the BV penalty: *en face* view of the target (Figure 9a) and of the optimal signals f^* defined on X (Figures 9b, 9c and 9d).

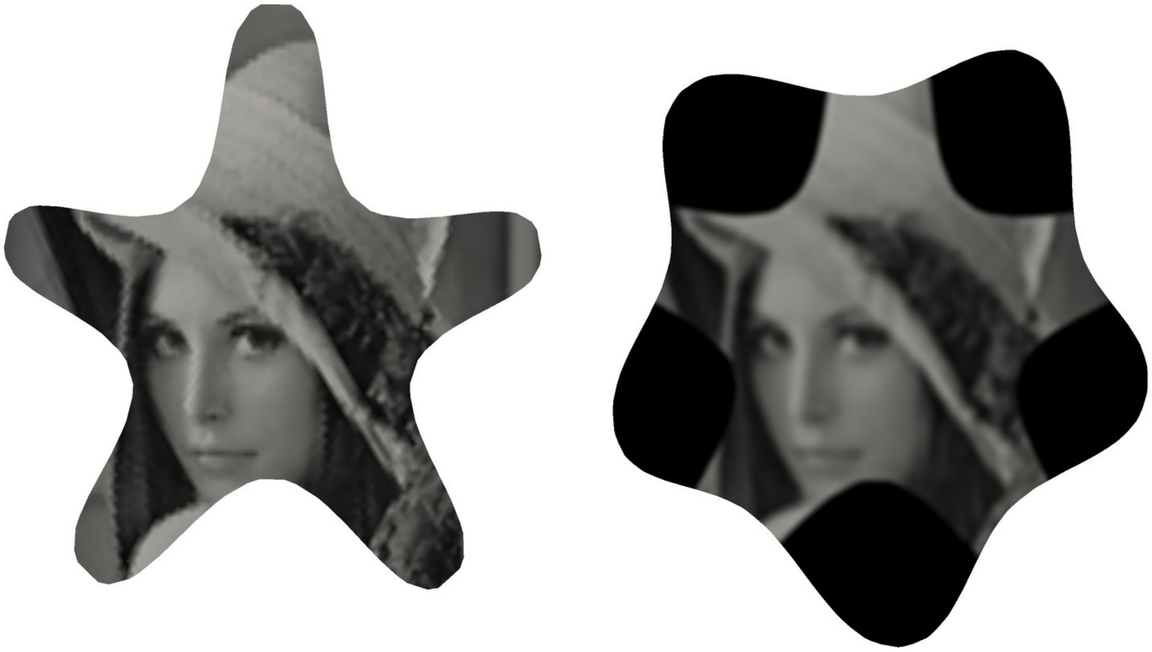

(a) The target (Y, g)

(b) $\alpha = 0.1$ and $\beta = 0.01$.

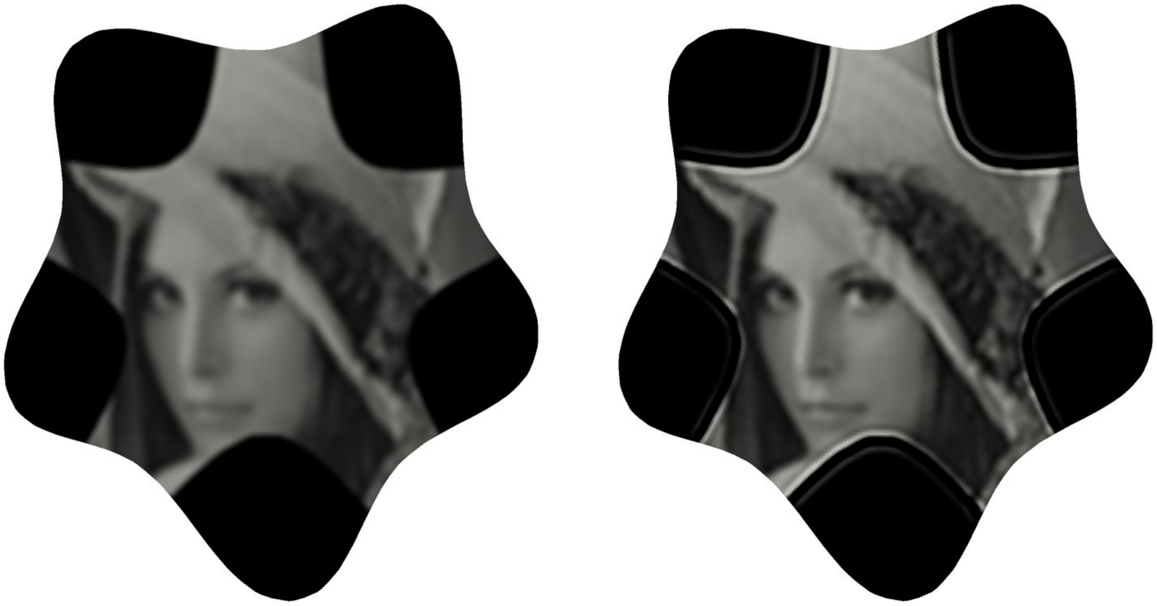

(c) $\alpha = 0.001$ and $\beta = 0.01$.

(d) $\alpha = 0.001$ and $\beta = 0.001$.

Figure 10: Results for the H^1 penalty: *en face* view of the target (Figure 10a) and of the optimal signals f^* defined on X (Figures 10b, 10c and 10d).

surfaces represent the lower boundary of the Nerves Fiber Layer (NFL) and the signals represent the thickness of the NFL. The variation of the thickness of the NFL may be an indicator of glaucoma. Considering Figure 11c or 12a (same scene from two different points of view), one can clearly see the misalignment of the two fshapes. This problem is very common in image analysis and the example of the smooth melting stars was a way to illustrate this problem.

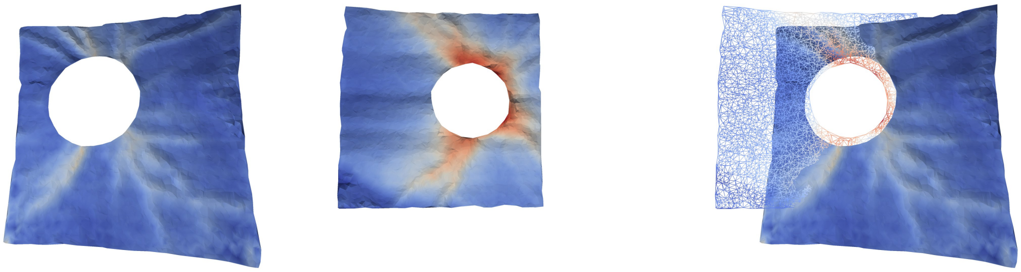
(a) Source data (X, f). (b) Target data (Y, g). (c) Relative position.

Figure 11: *En face* view of 2 particularly non-align individuals of the OCT dataset.

In practice, the usual transformations acting on fshapes are both geometric and functional as described in [6]. We then show some numerical results for the energy

$$E(f,\varphi) = pen(f) + pen(\varphi) + A(\varphi \cdot (X, f_0 + f), (Y, g)),$$

where

- $pen(\varphi)$ is the energy of the deformation $\varphi : \mathbb{R}^3 \to \mathbb{R}^3$ sending the source fshape on the target fshape. We use the Large Deformation Diffeomorphic Metric Mapping framework for fshapes (see [6]) to generate such a deformation and to compute its energy.
- $pen(f) = \begin{cases} \alpha \|f\|^2_{L^2(X)} & L^2 \text{ model} \\ \alpha \|f\|_{L^1(X)} + \beta |Df|(X) & BV \text{ model} \\ \alpha \|f\|^2_{L^2(X)} + \beta \|\nabla_X f\|^2_{L^2(X)} & H^1 \text{ model} \end{cases}.$

  The signal $f : X \to \mathbb{R}$ was called "functional residual" in [6] and is added to the original signal f_0 defined on X. The parameters α and β are positive constants.
- the attachment term is

  $$A(\varphi \cdot (X, f_0 + f), (Y, g)) = \gamma_W \left(\|\mu_{(\varphi(X), f_0+f)} - \mu_{(Y,g)}\|^2_{W'} + \|\mu_{(\varphi(\partial X), 0)} - \mu_{(\partial Y, 0)}\|^2_{W'} \right).$$

  It is a sum of two fvarifold terms: the first one involves the whole fshapes and the second one involves only the boundaries of the fshapes. This latter term enforces the matching of the boundaries and no signal is considered on the boundary. The parameter γ_W is a positive constant.

The optimum value for the deformation and the signal found after a gradient descent on E are denoted by φ^* and f^* respectively. The optimization in φ and f is performed simultaneously in

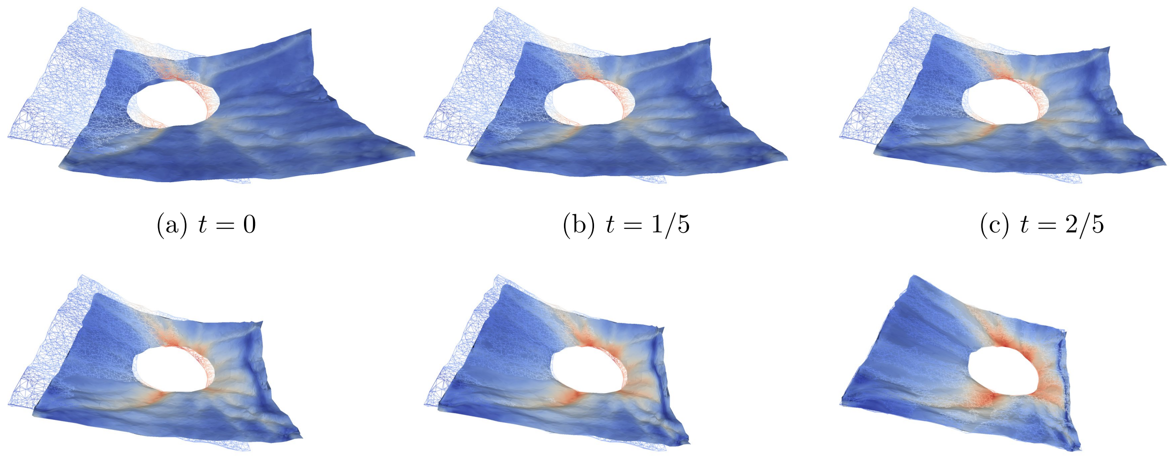

(a) $t = 0$

(b) $t = 1/5$

(c) $t = 2/5$

(d) $t = 3/5$

(e) $t = 4/5$

(f) $t = 1$

Figure 12: Perspective view of the geometric-functional shooting of the two fshapes presented Figure 11.

order to find a deformation φ^* taking the signal into account (*i.e.* matching loci with similar signal patterns together). In Figure 12 we show the results of the numerical experiment with the H^1 penalty.

In Figure 13, we show some results for the different models with a common γ_W and the best parameters α, β we were able to find for each model. We represent only the signal f^* found after the gradient descent and we do not discuss here the quality of the geometric matching. We can observe oscillating signal with the L^2 model. Regularizing the gradient of the penalty on f improve the quality of the result. Nevertheless, some low frequency oscillations are still present on the non overlapping part. The results with BV and H^1 model are much better as no oscillation may be observed. The H^1 model may be preferred on this example as the signal f^* has higher values.

8 Conclusion

Previous examples show the effects of a BV or H^1 penalties on the matching between fshapes and point out the quality of the results compared with the L^2 model. This is due essentially to the behavior of Gaussian kernels which can make the energy lower if the signal is oscillating (i.e., $|f_1 - f_2|$ large). The BV or H^1 models prevent from the oscillations and avoids uninteresting optimal solutions.

The paper takes into account the model with fixed geometry. A further problem concerns the study of the effects of the BV or H^1 penalties on the geometric evolutions. In the simultaneous optimization of the signal and geometry, the L^2-model can be trapped in poor optimal geometric configurations. The effects of the BV or H^1 models on these geometric phenomena has to be studied. The Γ-convergence for the global (geometry and signal) model is also to prove. These questions will be addressed in a future work.

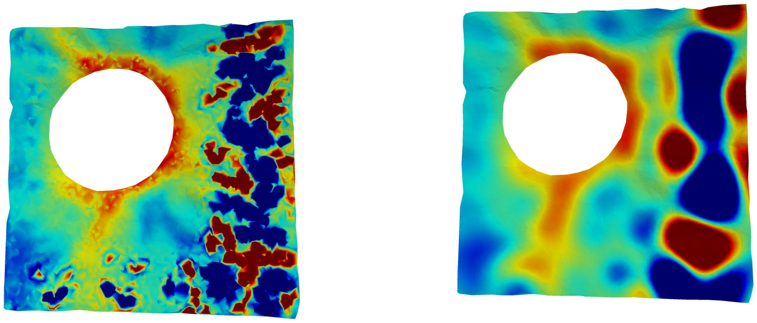

(a) L^2-model

(b) L^2-model (with regularized gradient descent)

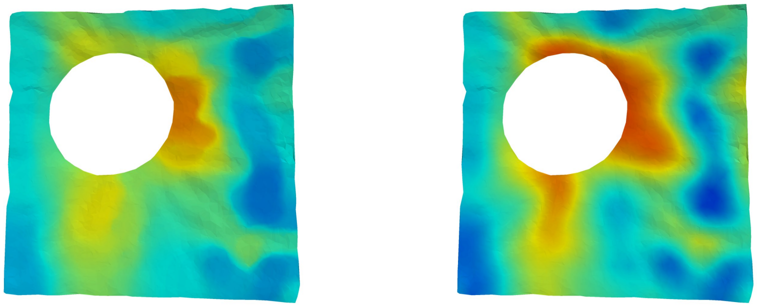

(c) BV model.

(d) H^1 model.

Figure 13: Optimal functional residuals (X, f^*) with the various penalty terms.

9 Appendix: functions of bounded variation on manifolds

9.1 Definitions and main properties

Here we consider a slightly more general framework where X is not supposed to be a finite 2D compact submanifold on $\mathbb{R}^3$ but a general compact d dimensional manifold. The definition of BV functions is however dependent of the introduction of a divergence operator (or equivalently of a volume form) and a local notion of length, two things that are provided by a Riemannian structure.

So, let X denotes a oriented smooth (at least C^1) compact d-dimensional Riemannian manifold possibly with boundary denoted ∂X and let vol_X be the associated Riemannian volume form. The boundary ∂X is supposed to be a C^1 compact $(d-1)$-dimensional manifold and we have $\mathrm{vol}_X(\partial X) = 0$. Finally, let us denote

$$X_0 \doteq X \setminus \partial X$$

which is a C^1 manifold without boundary. When X is without boundary, the previous construction gives $X_0 = X$. We say that $f \in L^1(X, \mathbb{R})$ is a function of bounded variation on X if

$$|D_X f|(X) \doteq \sup\left\{ \int_X f \mathrm{div}_X(u) \mathrm{vol}_X \mid u \in \chi_c^1(X_0),\ \|u\|_\infty \leqslant 1 \right\} < \infty$$

where $\chi^1_c(X_0)$ denotes the set of C^1 vector fields $u : X \to TX$ on X compactly supported in X_0 and div_X is the divergence operator on X defined by

$$\mathrm{div}_X(u) = \sum_{i=1}^{d} g(e_i, du(e_i))$$

where $(e_1, \cdots, e_d)$ is an orthonormal frame on TX. Here $\|u\|_\infty = \sup_{x\in X} g_x(u(x), u(x))^{\frac{1}{2}}$ where g is the metric tensor associated with the Riemannian structure. We recall the integration by part given Stokes formula :

$$\int_X h\mathrm{div}_X(u)\mathrm{vol}_X = -\int_X u(h)\mathrm{vol}_X = -\int_X g(\nabla h, u)\mathrm{vol}_X \tag{9.1}$$

where $h \in C^1_c(X_0)$ and $u(h)$ denotes the derivative of h along the vector fields u defined by $[u(h)](x) = d_x h(u(x))$ for any $x \in X_0$. Obviously we retrieve our previous submanifold setting when we consider the metric induce on the submanifold by the ambient space $\mathbb{R}^3$. In the other way, a much larger setting has been developed in a recent paper by Ambrosio et al. [4] that goes beyond our framework.

The functional space $BV(X)$ endowed with the norm

$$\|f\|_{BV(X)} = \|f\|_{L^1(X)} + |D_X f|(X)$$

is a Banach space.

Definition 9.1. The space $BV(X)$ can be also equipped with the following convergences, both weaker than the norm convergence:

1. **Weak-$*$ topology**. Let $\{f_n\} \subset BV(X)$ and $f \in BV(X)$. We say that the sequence $(f_n)_n$ weakly-$*$ converges in $BV(X)$ to f if

   $$f_n \overset{L^1(X)}{\longrightarrow} f \quad \text{and} \quad D_X f_n \overset{*}{\rightharpoonup} D_X f\,, \quad \text{as} \quad n \to \infty;$$

   where $\rightharpoonup$ denotes the weak convergence in the space of measure on X.

2. **Strict topology**. Let $\{f_n\} \subset BV(X)$ and $f \in BV(X)$. We say that the sequence $(f_n)_n$ strictly converges to f in $BV(X)$ if

   $$f_n \overset{L^1(X)}{\longrightarrow} f \quad \text{and} \quad |D_X f_n|(X) \longrightarrow |D_X f|(X)\,, \quad \text{as} \quad n \to \infty.$$

   Remark that the following distance

   $$d(f,g) = \|f-g\|_{L^1(X)} + \Big||D_X f|(X) - |D_X g|(X)\Big|$$

   is a distance in $BV(X)$ inducing the strict convergence.

We just recall that the strict convergence implies the weak-$*$ convergence (converse is not true). For more properties of functions of bounded variation we refer to [15, 3]. Functions of bounded variation on manifolds are studied in [4]. In the following we remind the main properties used in this paper and we adapt the proofs to the manifold case if necessary.

Proposition 9.2. A sequence $(f_n)_n$ in $BV(X)$ weakly-$*$ converges to f in $BV(X)$ if and only if $(f_n)_n$ is bounded in $BV(X)$ and converges to f in $L^1(X)$.

Proof. This is Proposition 3.13, page 125 in [3]. □

Finally, we remind the main compactness result for functions of bounded variation.

Theorem 9.3 (Compactness). Let $(f_n)_n$ be a sequence of $BV(X)$ such that $\|f_n\|_{BV(X)}$ is uniformly bounded. Then $\{f_n\}_n$ is relatively compact in $BV(X)$ with respect to the weakly-$*$ convergence.

Proof. The proof is similar to the classical-one (see Theorem 3.23 page 132 in [3]) and can be obtained by using a partition of the unity and the extension theorem like in the next section. □

9.2 Approximation by smooth $C^1(X_0)$-functions

In this section we establish an approximation result of BV functions by smooth functions. Interestingly, even if there exists several density results of smooth function using smoothing through the heat kernel semi-group for geodesically complete Riemannian manifold (see [18], [5] and [13]), to the best of our knowledge, an approximation result in the case of a compact manifold with boundary does not seem to be available. We give below such a result :

Theorem 9.4. Let X be a orientable Riemannian compact manifold with boundary ∂X and let $X_0 = X \setminus \partial X$. For any $h \in BV(X,\mathbb{R})$ there exist a sequence $h_n \in C^1(X_0,\mathbb{R})$ such that

$$\begin{cases} h_n \to h_{\restriction X_0} \text{ in } L^1(X_0,\mathbb{R}) \\ \text{and} \\ |D_X h|(X) = \lim_{n\to\infty} \int_{X_0} |\nabla h_n| \mathrm{vol}_X \,. \end{cases} \tag{9.2}$$

Our proof shares similar ideas than the proof of the classical approximation result in the case of an open set $\Omega \in \mathbb{R}^d$ (see Theorem 3.9 in [3]). However, the introduction of a non constant volume term when considering the problem in local charts introduces several new elements that need to be considered.

Proof. Let $(U_i)_{i\in I}$ be a finite atlas on X_0 and for any $1 \leqslant i \leqslant n$ let $\varphi_i : U_i \to V_i$ be a local chart such that $\overline{U_i}$ is compact and φ_i is the restriction to U_i of a C^1 diffeomorphisms from $\overline{U_i} \to \overline{V_i}$ (such an atlas exists since X is compact). Let $(\eta_j)_{j\geqslant 0}$ be a partition of unity such that $\mathrm{supp}(\eta_j)$ is compact for any $j \geqslant 0$ and there exists a partition $(J_i)_{1\leqslant i\leqslant n}$ of $\mathbb{N}$ for which $\mathrm{supp}(\eta_j) \subset U_i$ for any $j \in J_i$ which is locally finite on any U_i (i.e., for any $x \in U_i$, there exists an open set $U_i(x) \subset U_i$ such that $\mathrm{supp}(\eta_j) \cap U_i(x) = \varnothing$ for any $j \in J_i$ except on a finite number of j's).

For any $j \in J_i$ we consider ε_j such that $d(\varphi_i(\mathrm{supp}(\eta_j)), V_i^c) > \varepsilon_j$ and for $\boldsymbol{\varepsilon} = (\varepsilon_j)_{j\geqslant 0}$ we consider the linear operator $L_{\boldsymbol{\varepsilon}} : BV(X,\mathbb{R}) \to C^1(X_0,\mathbb{R})$ defined by

$$L_{\boldsymbol{\varepsilon}} h \doteq \sum_{i=1}^{n} \varphi_i^* \Big(\sum_{j\in J_i} \psi_i^*(h\eta_j) * \rho_{\varepsilon_j} \Big)$$

where $\psi_i : V_i \to U_i$ is the inverse mapping of φ_i. Note that we are using here classical notation of differential geometry for pullbacks where for any function $\ell \in C_c(U_i,\mathbb{R})$, $\psi_i^*\ell \doteq \ell \circ \psi_i$ and for any $v \in \chi_c^1(U_i)$, $\psi_i^* v = (d\psi_i)^{-1} v \circ \psi_i$. Eventually, on every V_i, we introduce $\alpha_i dx$ the pullback of $\mathrm{vol}_{X\restriction U_i}$ by ψ_i on V_i such that for any $\ell \in C_c(U_i)$, we have $\int_{U_i} \ell \mathrm{vol}_X = \int_{V_i} (\psi_i^*\ell)\alpha_i dx$.

Let $\delta > 0$. We can assume that for any $1 \leqslant i \leqslant n$ and any $j \in J_i$, we have ε_j small enough so that

$$\int_{V_i} |\psi_i^*(h\eta_j) * \rho_{\varepsilon_j} - \psi_i^*(h\eta_j)| \alpha_i dx \leqslant \delta 2^{-j} \,.$$

Since $(\eta_j)_{j\geqslant 0}$ is a partition of unity, we have $h=\sum\limits_{i=1}^{n}\sum\limits_{j\in J_i} h\eta_j$ and

$$\int_X |L_\varepsilon h - h|\mathrm{vol}_X \leqslant \sum_{i=1}^{n}\int_{V_i}\sum_{j\in V_j}|\psi_i^*(h\eta_j)*\rho_{\varepsilon_j}-\psi_i^*(h\eta_j)|\alpha_i dx \leqslant 2\delta\,. \tag{9.3}$$

This first inequality is enough to prove an approximation result in a L^1 sense. We turn now to the control of the total variation part.

Let $u\in\chi_c^1(X_0)$. We have the following decomposition using the integration by part formula (9.1) for equality (a) and the classical integration by part on $\mathbb{R}^d$ for equality (b)

$$\begin{aligned}
\int_X L_\varepsilon h \mathrm{div}_X(u)\mathrm{vol}_X &= \sum_{i=1}^{n}\int_X \varphi_i^*\Big(\sum_{j\in J_i}\psi_i^*(h\eta_j)*\rho_{\varepsilon_j}\Big)\mathrm{div}_X(u)\mathrm{vol}_X\\
&\overset{(a)}{=} -\sum_{i=1}^{n}\int_X u\Big(\varphi_i^*\Big(\sum_{j\in J_i}\psi_i^*(h\eta_j)*\rho_{\varepsilon_j}\Big)\Big)\mathrm{vol}_X\\
&= -\sum_{i=1}^{n}\int_{V_i}\sum_{j\in J_i}(\psi_i^*u)\Big(\sum_{j\in J_i}\psi_i^*(h\eta_j)*\rho_{\varepsilon_j}\Big)\alpha_i dx\\
&\overset{(b)}{=} \sum_{i=1}^{n}\int_{V_i}\sum_{j\in J_i}[\psi_i^*(h\eta_j)]*\rho_{\varepsilon_j}\mathrm{div}(\alpha_i\psi_i^*u)dx\\
&= \sum_{i=1}^{n}\int_{V_i}\sum_{j\in J_i}\psi_i^*(h\eta_j)\mathrm{div}([\alpha_i\psi_i^*u]*\rho_{\varepsilon_j})dx\\
&= \sum_{i=1}^{n}\underbrace{\int_{V_i}\sum_{j\in J_i}\psi_i^*(h)\mathrm{div}(\psi_i^*\eta_j([\alpha_i\psi_i^*u]*\rho_{\varepsilon_j}))dx}_{A_{ij}}\\
&\qquad -\sum_{i=1}^{n}\underbrace{\int_{V_i}\sum_{j\in J_i}\psi_i^*(h)([\alpha_i\psi_i^*u]*\rho_{\varepsilon_j})(\psi_i^*\eta_j)dx}_{B_{ij}}
\end{aligned}$$

with

$$A_{ij}=\int_{V_i}\sum_{j\in J_i}\psi_i^*(h)\left[\mathrm{div}\Big(\alpha_i\psi_i^*\eta_j((\psi_i^*u)*\rho_{\varepsilon_j})\Big)+\mathrm{div}\Big(\psi_i^*\eta_j([\alpha_i\psi_i^*u]*\rho_{\varepsilon_j}-\alpha_i[(\psi_i^*u)*\rho_{\varepsilon_j}])\Big)\right]dx\,.$$

However, for any $\delta>0$, denoting $|\cdot|_x$ the norm at $x\in X$ induced by the metric we have for $x\in\mathrm{supp}(\eta_j)$

$$\begin{aligned}
&|\varphi_i^*((\psi_i^*u)*\rho_{\varepsilon_j})|_x(x)\\
&\qquad=\left|(d_x\varphi_i)^{-1}\Big(\int_{V_i}d_{\psi_i(\varphi_i(x)-y)}\varphi_i u(\psi_i(\varphi_i(x)-y))\rho_{\varepsilon_j}(y)dy\Big)\right|_x\\
&\qquad\leqslant 1+\left|(d_x\varphi_i)^{-1}\Big(\int_{V_i}(d_{\psi_i(\varphi_i(x)-y)}\varphi_i-d_x\varphi_i)u(\psi_i(\varphi_i(x)-y))\rho_{\varepsilon_j}(y)dy\Big)\right|_x\\
&\qquad\leqslant 1+\delta
\end{aligned}$$

for ε_j small enough uniformly in u such that $\|u\|_\infty \leqslant 1$ and $j \in J_i$. Hence

$$\begin{aligned}\sum_{i=1}^{n}\left|\int_{V_i}\sum_{j\in J_i}\psi_i^*(h)\mathrm{div}(\alpha_i\psi_i^*\eta_j((\psi_i^*u)*\rho_{\varepsilon_j}))dx\right| &\leqslant \sum_i\int_X\sum_{j\in J_i}\eta_j(1+\delta)d|D_Xh| \\ &\leqslant (1+\delta)|D_Xh|(X)\,.\end{aligned} \tag{9.4}$$

Moreover, we can assume for ε_j small enough we have for $x \in \mathrm{supp}(\eta_j)$

$$\begin{aligned}&\left|\varphi_i^*\frac{[\alpha_i\psi_i^*u]*\rho_{\varepsilon_j}-\alpha_i[(\psi_i^*u)*\rho_{\varepsilon_j}]}{\alpha_i}\right|_x \\ &\quad=\left|d_x\varphi_i^{-1}\int_{V_i}\frac{\alpha_i(\varphi_i(x)-y)-\alpha_i(\varphi_i(x))}{\alpha_i(\varphi_i(x))}d_{\psi(\varphi_i(x)-y)}\varphi_i u(\psi_i(\varphi_i(x)-y))\rho_{\varepsilon_j}(y)dy\right|_x \leqslant \delta\end{aligned}$$

so that

$$\begin{aligned}&\sum_{i=1}^{n}\left|\int_{V_i}\sum_{j\in J_i}\psi_i^*h\mathrm{div}\Big(\alpha_i\psi_i^*\eta_j\frac{[\alpha_i\psi_i^*u]*\rho_{\varepsilon_j}-\alpha_i[(\psi_i^*u)*\rho_{\varepsilon_j}]}{\alpha_i}\Big)dx\right| \\ &\quad\leqslant \sum_i\int_X\sum_{j\in J_i}\eta_j\delta|D_Xh| \leqslant \delta|D_Xh|(X)\end{aligned} \tag{9.5}$$

Thus we have

$$\sum_{i=1}^{n}A_{ij} \leqslant |D_Xh|(X)(1+2\delta)\,. \tag{9.6}$$

Let us consider now the B_{ij}'s. We have

$$\begin{aligned}B_{ij} &= \int_{V_i}\Big\langle\int_{V_i}(\alpha_i\psi_i^*u)(x-y)\rho_{\varepsilon_j}(y)dy, \Big(\psi_i^*h\nabla(\psi_i^*\eta_j)\Big)(x)\Big\rangle dx \\ &= \int_{V_i}\Big\langle(\alpha_i\psi_i^*u)(x), \int_{V_j}\Big(\psi_i^*h\nabla(\psi_i^*\eta_j)\Big)(x-y)\rho_{\varepsilon_j}(y)dy\Big\rangle dx \\ &= \underbrace{\int_{V_i}\alpha_i\psi_i^*h\psi_i^*u(\psi_i^*\eta_j)dx}_{B_{ij}^1}+\underbrace{\int_{V_i}\Big\langle(\alpha_i\psi_i^*u)(x),(\psi_i^*h\nabla(\psi_i^*\eta_j))*\rho_{\varepsilon_j}-\psi_i^*h\nabla(\psi_i^*\eta_j)\Big\rangle dx}_{B_{ij}^2}\,.\end{aligned} \tag{9.7}$$

Concerning the B_{ij}^1 terms, we have

$$\sum_{i=1}^{n}\sum_{j\in J_j}B_{ij}^1 = \sum_{i=1}^{n}\int_X\sum_{j\in J_j}hu(\eta_j)\mathrm{vol}_X = \int_X hu(1)\mathrm{vol}_X = 0. \tag{9.8}$$

For the B_{ij}^2 terms, let us notice that $\sup_{V_i}|\alpha_i\psi_i^*u| < \infty$ uniformly in u (since $\|u\|_\infty \leqslant 1$) and $(\psi_i^*h\nabla(\psi_i^*\eta_j))*\rho_{\varepsilon_j} \to (\psi_i^*h\nabla(\psi_i^*\eta_j))$ in $L^1(\mathbb{R}^d, dx)$ so that for ε_j sufficiently small, we can assume that $|B_{ij}^2| \leqslant \delta 2^{-(j+1)}$. Summing along the indices, we get

$$\left|\sum_{i=1}\sum_{j\in J_i}B_{ij}^2\right| \leqslant \delta \tag{9.9}$$

and with (9.6), (9.8) and (9.9) we get eventually that for sufficiently small values of the ε_j's we have uniformly in $u \in \chi_c^2(X_0)$ satisfying $\|u\|_\infty \leqslant 1$

$$\left|\int_X L_\varepsilon h\mathrm{div}_X(u)\mathrm{vol}_X\right| \leqslant |D_Xh|(X)(1+2\delta+\delta^2)+\delta\,. \tag{9.10}$$

Taking the supremum over such u, we get

$$|D_X L_\varepsilon h|(X) \leqslant |D_X h|(X)(1 + 2\delta + \delta^2) + \delta. \tag{9.11}$$

Since δ is arbitrary we have shown that there exists a sequence $(\varepsilon_k)_{k\geqslant 0}$ such that $L_{\varepsilon_k} h \in C^\infty(X_0)$,

$$\limsup_k |D_X L_{\varepsilon_k} h|(X) \leqslant |D_X h|(X)\,. \tag{9.12}$$

Moreover, since we can assume that $L_{\varepsilon_k} h \to h$ in $L^1(X)$, we get from the lower semi-continuity of the total variation in L^1 that $L_{\varepsilon_k} h \to h$ for the S-topology. □

9.3 Approximation by $C^1(X)$-functions

We can improve the previous result by showing an approximation result by $C^1(X)$-functions. To this end we define an extension of the manifold and we extend the function f to such a larger manifold. Then, we can obtain the needed approximation by a suitable approximation of the extended function. We give the details in the following.

In the following X denotes a C^p ($p \geqslant 2$) compact oriented 2 dimensional submanifold of $\mathbb{R}^3$ with non empty boundary denoted ∂X. We denote $\boldsymbol{n}_{X_0}$ the C^{p-1} vectors field of positively oriented normal along $X_0 = X \setminus \partial X$. Note that $\boldsymbol{n}_{X_0}$ can be continuously extended on X and denoted in that case $\boldsymbol{n}_X$. Thence, for any $x \in \partial X$ we can define the unit vector $\nu(x)$ pointing outward and orthogonal to both $n_X(x)$ and ∂X. For sufficiently small $r > 0$, the subset $\mathcal{N}_r(X_0)$ defined by (4.3) is a open set on such that the mapping

$$\psi_{X_0} : (x, t) \mapsto x + t\boldsymbol{n}_{X_0}(x)$$

is a C^{p-1} diffeomorphism from $X_0 \times]-r, r[$ to $\mathcal{N}_r(X_0)$ so that considering its inverse $\psi_{X_0}^{-1} = (\pi_{X_0}, t_{X_0})$ we have

$$z = \pi_{X_0}(z) + t_{X_0}(z)\boldsymbol{n}_{X_0}(\pi_{X_0}(z))$$

for $z \in \mathcal{N}_r(X_0)$ and $\pi_{X_0}(z)$ can be interpreted as the orthonormal projection of z on X_0 and $|t_{X_0}(z)|$ as the distance from z to X_0. Now there exists $\eta_0 > 0$ small enough such that the mapping $\mathrm{Ext} : \partial X \times] - \eta_0, \eta_0[\times] - r, r[\to \mathbb{R}^3$ such that

$$\mathrm{Ext}(x, s, t) = \begin{cases} x_0 + t\boldsymbol{n}_{X_0}(x_0) \text{ with } x_0 \doteq \pi_{X_0}(x + s\nu(x)) & \text{if } s < 0 \\ x + s\nu(x) + t\boldsymbol{n}_X(x) & \text{otherwise} \end{cases} \tag{9.13}$$

is well defined and is a C^{p-1} diffeomorphism on an open neighborhood of ∂X in $\mathbb{R}^3$ (see Figure 14).

Moreover, Ext maps $\partial X \times \{0\} \times \{0\}$ to the boundary ∂X of X and for $0 < \eta < \eta_0$ if

$$X^{-\eta} \doteq X \setminus \mathrm{Ext}(\partial X \times] - \eta, 0] \times \{0\})$$

$X^{-\eta}$ is a compact C^{p-1} submanifold of X whereas

$$X^{+\eta} \doteq X \cup \mathrm{Ext}(\partial X \times]0, +\eta] \times \{0\}) \tag{9.14}$$

is a C^{p-1} compact 2 dimensional submanifold of $\mathbb{R}^3$ extending X along its boundary.

Next theorem proves an approximation result by using $C^{p-1}(X)$-functions.

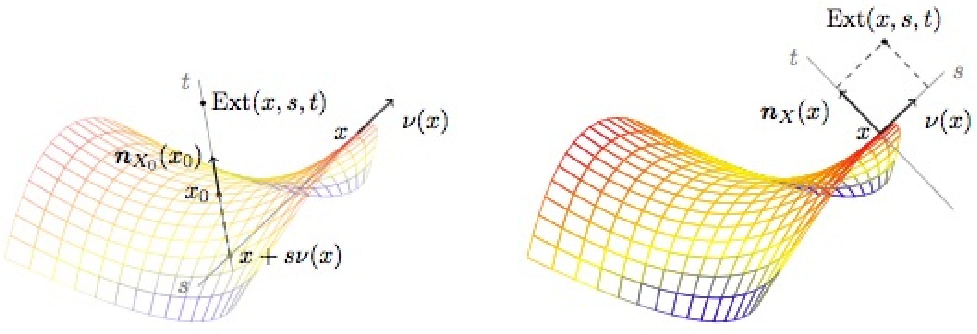

(a) $s < 0$ (b) $s \geqslant 0$

Figure 14: The map Ext

Theorem 9.5. Let X be a C^p ($p \geqslant 2$) compact oriented 2D submanifold of $\mathbb{R}^3$ with non empty boundary denoted ∂X. Let $f \in BV(X, \mathbb{R})$ and let $\varepsilon > 0$. Then there exists $\eta > 0$ and $\tilde{f} \in C^{p-1}(X^{+\eta}, \mathbb{R}^d)$ such that

$$\int_X |f - \tilde{f}| \, d\mathcal{H}^2 + \Big| |D_X f|(X) - |D_X \tilde{f}|(X) \Big| \leqslant \varepsilon$$

and

$$\int_{X^{+\eta} \setminus X^{-\eta}} |\tilde{f}| + |\nabla_{X^{+\eta}} \tilde{f}| \, d\mathcal{H}^2 \leqslant \varepsilon \, .$$

Proof. We have first the existence of $f' \in C^{p-1}(X_0, \mathbb{R})$ such that

$$\int_X |f - f'| \, d\mathcal{H}^2 + \Big| |D_X f|(X) - |D_X f'|(X) \Big| \leqslant \varepsilon \, .$$

Moreover, there exists $0 < \eta' < \eta_0$ such that

$$\int_{X \setminus X^{-\eta'}} |f'| + |\nabla_X f'| \, d\mathcal{H}^2 \leqslant \varepsilon$$

Now, consider for $\eta = \eta'/3$ the function $f'' : X^{+\eta} \to \mathbb{R}$ defined as

$$f''(z) = \begin{cases} f(z) & \text{if } z \in X^{-\eta} \\ f(\mathrm{Ext}(x, -2\eta - s, 0)) & \text{if } z \in X^{+\eta} \setminus X^{-\eta} \text{ and where } z = \mathrm{Ext}(x, s, 0) \end{cases}$$

Let $\delta > 0$, we check easily that for η' small enough

$$\int_{X^{+\eta} \setminus X^{-\eta}} |f''| + |\nabla_X f''| \, d\mathcal{H}^2 \leqslant (1 + \delta) \times 2 \int_{X \setminus X^{-\eta'}} |f'| + |\nabla_X f'| \, d\mathcal{H}^2$$

since considering the change of variable induced by Ext we notice that $(x, s) \to \pi_X(x + s\nu(x))$ has a determinant converging to 1 when (x, s) convergence to a point on $\partial X \times \{0\}$ with $s < 0$. Moreover, we check easily that $f''\restriction_{X^{-\eta}} \in C^{p-1}(X^{-\eta})$ and $f''\restriction_{\overline{X^{+\eta} \setminus X^{-\eta}}} \in C^{p-1}(\overline{X^{+\eta} \setminus X^{-\eta}})$ where the intersection $X^{-\eta} \cap \overline{X^{+\eta} \setminus X^{-\eta}} = \partial X^{-\eta}$ is a C^{p-1} one dimensional submanifold. Applying a smoothing in the vicinity of $\partial X^{-\eta}$ we can obtain $\tilde{f} \in C^1(X^{+\eta}, \mathbb{R})$ such that $\tilde{f} = f''$ on $X^{-\eta}$ and

$\int_{X^{+\eta}\setminus X^{-\eta}} |\tilde{f}| + |\nabla_X \tilde{f}| \, d\mathcal{H}^2 \leqslant \int_{X^{+\eta}\setminus X^{-\eta}} |f''| + |\nabla_X f''| \, d\mathcal{H}^2 + \varepsilon$ so that (choosing $\delta = 1$ and η' small enough)

$$\int_{X^{+\eta}\setminus X^{-\eta}} |\tilde{f}| + |\nabla_X \tilde{f}| \, d\mathcal{H}^2 \leqslant 5\varepsilon$$

We get immediately

$$\int_X |f - \tilde{f}| \, d\mathcal{H}^2 + \Big| |D_X f|(X) - |D_X \tilde{f}|(X) \Big| \leqslant \int_X |f - f'| \, d\mathcal{H}^2 + \Big| |D_X f|(X) - |D_X f'|(X) \Big| + 5\varepsilon \leqslant 6\varepsilon$$

and the result is proven. □

Remark 9.6 (**L^2 and H^1 norms).** Theorems 9.4 and 9.5 can also be stated by using the L^2 and H^1 norms instead of the BV-one. The proofs in this case are simpler and follow the same argument than the previous ones.

References

[1] A.D.Alexandrov and V.A.Zalgaller. Intrinsic geometry of surfaces,. *Translation of Mathematical Monographs. AMS*, 15, 1967.

[2] Grégoire Allaire. *Numerical analysis and optimization: an introduction to mathematical modelling and numerical simulation.* Numerical Mathematics and Scientific Computation. Oxford Univ. Press, New York, NY, 2007.

[3] L. Ambrosio, N. Fusco, and D. Pallara. Functions of Bounded Variation and Free Discontinuity Problems. *Oxford Science Publications*, 2000.

[4] L. Ambrosio, R. Ghezzi, and V. Magnani. BV functions and set of finite perimeter in sub-Riemannian manifolds. *http://arxiv.org/abs/1303.6074*, 2013.

[5] Andrea Carbonaro and Giancarlo Mauceri. A note on bounded variation and heat semigroup on riemannian manifolds. *Bulletin of the Australian Mathematical Society*, 76(01):155–160, 2007.

[6] B. Charlier, N. Charon, and A.Trouvé. The fshape framework for the variability analysis of functional shapes. *Submitted*, 2014.

[7] B. Charlier, N. Charon, G. Nardi, and A. Trouvé. `FshapesTk`: Functional shapes toolkit. `https://github.com/fshapes/fshapesTk`, 2011–2015.

[8] N. Charon and A. Trouvé. The varifold representation of non-oriented shapes for diffeomorphic registration. *SIAM Journal on Imaging Science*, 6(4):2547–2580, 2013.

[9] P.G. Ciarlet. The Finite Elements Method for Elliptic Problems. *SIAM, Classics in Applied Mathematics*, 40, 2002.

[10] H. Federer. Curvature measures. *Trans. Amer. Math. Soc.*, 93:418–491, 1959.

[11] G.Dziuk. Finite elements for the Beltrami operator on arbitrary surfaces. *Partial Differential Equations and Calculus of Variations (S. Hildebrandt and R. Leis, eds), Vol. 1357 of Lecture Notes in Mathematics, Springer*, pages 142–155, 1988.

[12] J. Glaunès and M. Vaillant. Surface matching via currents. *Proceedings of Information Processing in Medical Imaging (IPMI), Lecture Notes in Computer Science*, 3565:381–392, 2006.

[13] Batu Güneysu and Diego Pallara. Functions with bounded variation on a class of riemannian manifolds with ricci curvature unbounded from below. *Mathematische Annalen*, pages 1–25, 2013.

[14] R. L. Jerrard and P. Sternberg. Critical points via Gamma-convergence: general theory and applications. *Jour. Eur. Math. Soc.*, 11 (4):705–753, 2009.

[15] L.C.Evans and R.F. Garipey. Measure Theory and Fine Properties of Functions. *CRC Press*, 1992.

[16] S. Lee, N. Fallah, F. Forooghian, A. Ko, K. Pakzad-Vaezi, A.B. Merkur, A.W. Kirker, D.A Albiani, M. Young, M.V. Sarunic, and M.F. Beg. Comparative analysis of repeatability of manual and automated choroidal thickness measurements in nonneovascular age-related macular degeneration. *Investigative Ophthalmology and Vision Science*, 53(5):2864–2871, 2013.

[17] S. Lee, M. Young, M.F. Beg, and M.V. Sarunic P.J. Mackenzie. Comparative analysis of repeatability of manual and automated choroidal thickness measurements in nonneovascular age-related macular degeneration. *preprint*, 2014.

[18] Mi Miranda, Diego Pallara, Fabio Paronetto, and Marc Preunkert. Heat semigroup and functions of bounded variation on riemannian manifolds. *Journal für die reine und angewandte Mathematik (Crelles Journal)*, 2007(613):99–119, 2007.

[19] J.-M. Morvan and B. Thibert. Approximation of the normal vector field and the area of a smooth surface. *Discrete Comput Geom*, 32:383–400, 2004.

[20] K. Polthier and M. Schmies. Straightest geodesics on polyhedral surfaces. *Procceding SIIGRAPH'06*, pages 30–38, 2006.

[21] Y.G Reshetnyak. Geometry IV. *Encyclopaedia of Mathematical Sciences. Springer Verlag, ch. 1. TwoDimensional Manifolds of Bounded Curvature*, 70:3–164, 1993.

[22] L. Simon. Lectures on Geometric Measure Theory. *Proceedings of the Centre for mathematical analysis, Australian National University*, 3, 1983.

[23] M. Spivak. A Comprehensive Introduction to Differential Geometry. *Publish or Perish, Inc., Houston, Texas*, Vol. 1, 1999.

[24] L. Younes. Shapes and Diffeomorphisms. *Springer, Applied Mathematical Science*, 171, 2010.